# Accepted Manuscript


Novel nannocystin A analogues as anticancer therapeutics: Synthesis, biological evaluations and structure–activity relationship studies

Qiang Liu, Xiaohong Yang, Jie Ji, Shao-Lin Zhang, Yun He

PII: S0223-5234(19)30222-3

DOI: https://doi.org/10.1016/j.ejmech.2019.03.011

Reference: EJMECH 11181

To appear in: *European Journal of Medicinal Chemistry*

Received Date: 16 January 2019

Revised Date: 22 February 2019

Accepted Date: 5 March 2019

Please cite this article as: Q. Liu, X. Yang, J. Ji, S.-L. Zhang, Y. He, Novel nannocystin A analogues as anticancer therapeutics: Synthesis, biological evaluations and structure–activity relationship studies, *European Journal of Medicinal Chemistry* (2019), doi: https://doi.org/10.1016/j.ejmech.2019.03.011.

## Graphical Abstract

A structurally simplified nannocystin A analogue **LQ18** exhibited potent antiproliferative activities with $IC_{50}$ values ranging from 4.3 to 48 nM against tested cancer cell lines, and inhibited eEF1A1 expression in A549 cell line.

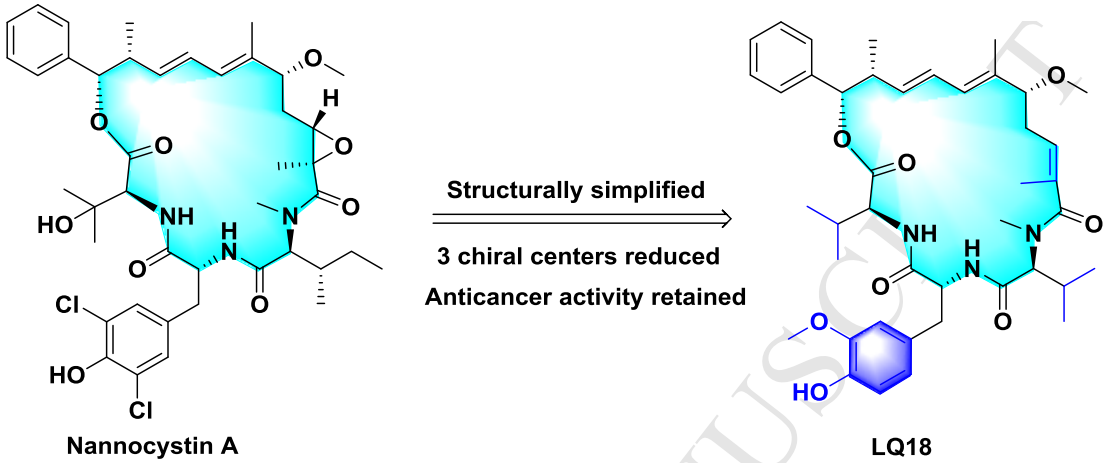

**Title page**

**Title:**

Novel nannocystin A analogues as anticancer therapeutics: synthesis, biological evaluations and structure–activity relationship studies

**Author names and affiliations:**

Qiang Liu[#], Xiaohong Yang[#], Jie Ji, Shao-Lin Zhang*, Yun He*

*School of Pharmaceutical Sciences, Chongqing Key Laboratory of Natural Product Synthesis and Drug Research, Chongqing University, Chongqing, 401331, P. R. China*

* Corresponding address:

Tel.: +86-23-65678465; E-mail: zhangsl@cqu.edu.cn; yun.he@cqu.edu.cn

[#]: These authors contributed equally.

**Abstract:**

Nannocystin A is a novel 21-membered macrocyclic lactam that targets eukaryotic translation elongation factor 1α (eEF1A) and displays potent antiproliferative activities. Herein, a series of nannocystin A analogues were synthesized and their structure–activity relationship (SAR) were established based on the MTT assay and western blotting analysis. The SAR enabled us to identify a structurally simplified nannocystin A analogue **LQ18**, which exhibited potent antiproliferative activities with $IC_{50}$ values ranging from 4.3 to 48 nM against the tested cell lines, and inhibited eEF1A1 expression in A549 cell line. **LQ18** arrested cell cycle at G2 phase and induced A549 cell apoptosis *via* up-regulation of caspase-3, caspase-9 and bax protein expressions in a dose-dependent manner, while it significantly decreased the bcl-2 expression. Collectively, these data demonstrated that **LQ18** could be a promising lead for the development of structurally novel eEF1A1 inhibitor for cancer treatment.

***Keywords*:** Nannocystin A, anticancer, SAR study

## 1. Introduction

Natural products are the most proliferative source of leads and / or drug candidates in drug development [1]. Natural products from plants, microbes, and animals, as well as synthetic or semi-synthetic compounds have continued to advance into clinical trials, particularly in anticancer and antimicrobial fields [2, 3]. An analysis of the new drugs approved by the US Food and Drug Administration (FDA) between 1981 and 2010 suggested that 34% of those drugs were natural products or direct derivatives from natural products [4]. Thus drug discovery based on natural products is becoming increasingly popular in recent years.

In 2015, Brönstrup *et. al.* [5] and Hoepfner *et. al.* [6] independently disclosed the isolation of nannocystin A from the myxobaterium *Nannocystis sp*. Its relative and absolute configurations were then confirmed by extensive NMR spectroscopic analysis and furtherer established by a single-crystal X-ray analysis [6], which suggest that nannocystin A (**Fig. 1**) is a 21-membered macrocycle containing both peptide and polyketide fragments, and possesses nine stereogenic centers in the carbon backbone.

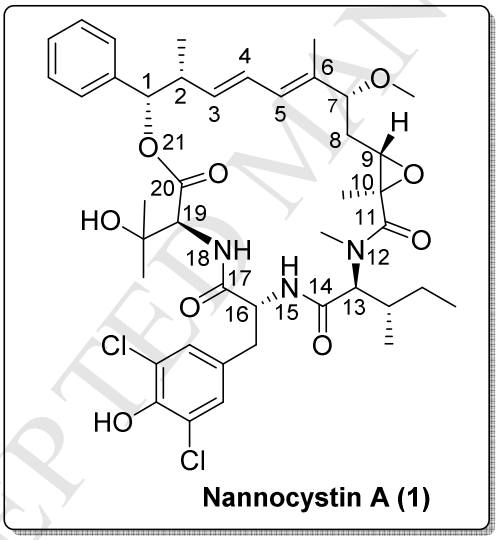


**Fig. 1** Chemical structure of nannocystin A

Nannocystin A potently inhibited various cancer cell lines at nanomolar concentrations, the $IC_{50}$ values are 1.0 and 12 nM for PC3 and HL60 cells, respectively [5]. Its antiproliferative activities probably resulted from the inhibition of eukaryotic translation elongation factor 1-α 1 (eEF1A1), which regulates the ribosomal protein synthesis and involves in cytoskeletal organization and other physiological activities [7, 8]. In addition, eEF1A1 is associated with the development and progression of various human cancers [9, 10] and has thus been proposed as a target for anticancer therapy [11]. However, no drug based on this target has been successfully marketed. Moreover, the overexpression or depletion of eEF1A1 has been shown to influence the rate of cancer cell apoptosis. Collectively, these studies suggested that eEF1A1 was an attractive anticancer target,

the inhibition of eEF1A1 protein could provide a promising approach for killing or, at least, greatly reducing the growth of cancer cells.

Previously, our laboratory [12] and others completed the total synthesis of nannocystin A [13-15], and some nannocystin A analogues were also disclosed [16, 17]. However, the systematical modification of nannocystin A and its detailed SAR studies are limited. Continuing our efforts in discovering novel therapeutics based on natural and designed products [18-23], herein we report the optimization, biological evaluation, and SAR analysis of a series of novel nannocystin A analogues.

## 2. Results and discussion

### 2.1 Chemistry

The retrosynthetic analysis of nannocystin A was outlined in **Scheme 1**, which could be assembled from three main fragments, A, B and C, respectively. The structures of each fragment used in our study were listed in **Table 1**, which were individually synthesized and optimized. With the diverse set of fragments in hand, nannocystin A analogues were conveniently assembled (**Table 2**).

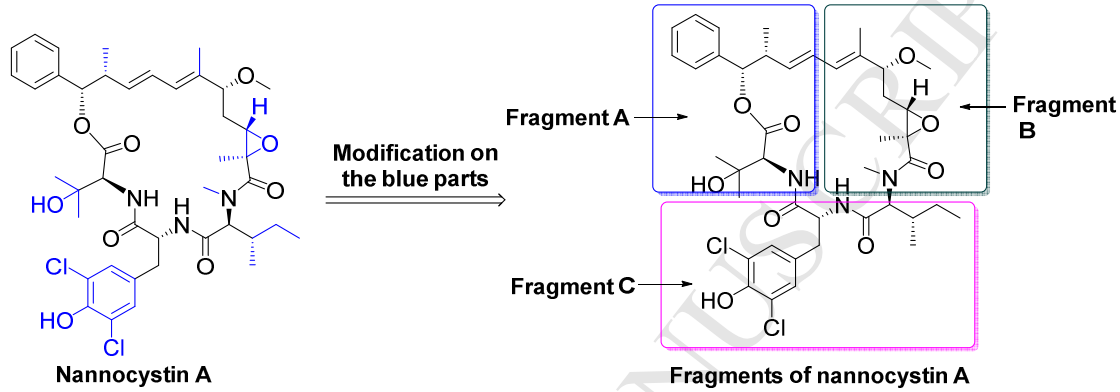


**Scheme 1** Retrosynthetic analysis for the construction of nannocystin A

**Table 1** Structures of fragments A, B and C

| | | | | | |
|---|---|---|---|---|---|
| Fragment A | 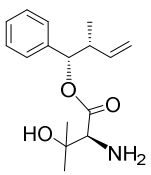 **A1** | 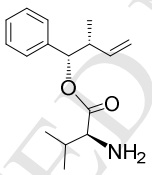 **A2** | 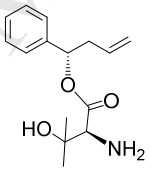 **A3** | 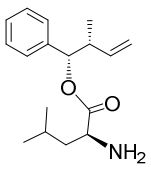 **A4** | 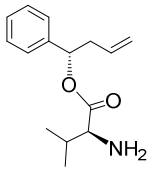 **A5** |
| Fragment B | 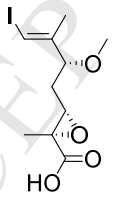 **B1** | 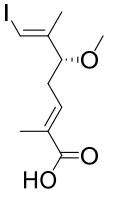 **B2** | 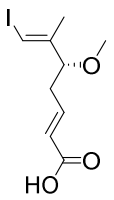 **B3** | 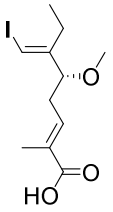 **B4** | |
| Fragment C | 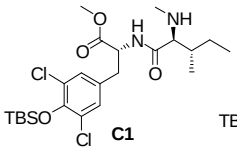 **C1** | 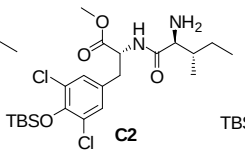 **C2** | 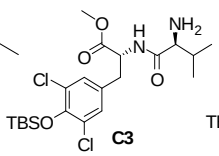 **C3** | 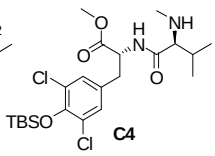 **C4** | |
| | 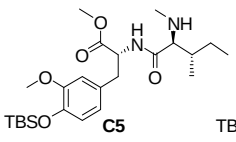 **C5** | 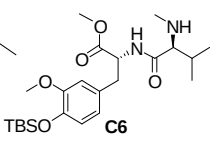 **C6** | 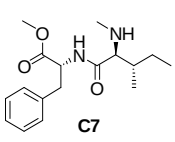 **C7** | 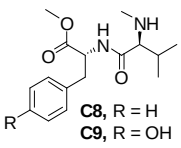 **C8,** R = H **C9,** R = OH | |

As shown in **Scheme 2**, the synthesis of fragments **A1**, **A2**, **A4** started from known alcohol **2** [24], which was oxidized *via* PCC, then followed by Witting reaction to afford olefin **3** in 70% yield [25]. Deprotection of the TBS group in **3** with TBAF gave rise to alcohol **4** in 95% yield. Subsequent esterification with acids **5**, **6** or **7** respectively provided the corresponding esters in 68-80% yields. After treating with TFA or TBAF, amine fragments **A1**, **A2** and **A4** were isolated in 80-90% yields. Amines **A3** and **A5** were synthesized from known alcohol **8**, which was prepared according to the literature procedures [26].

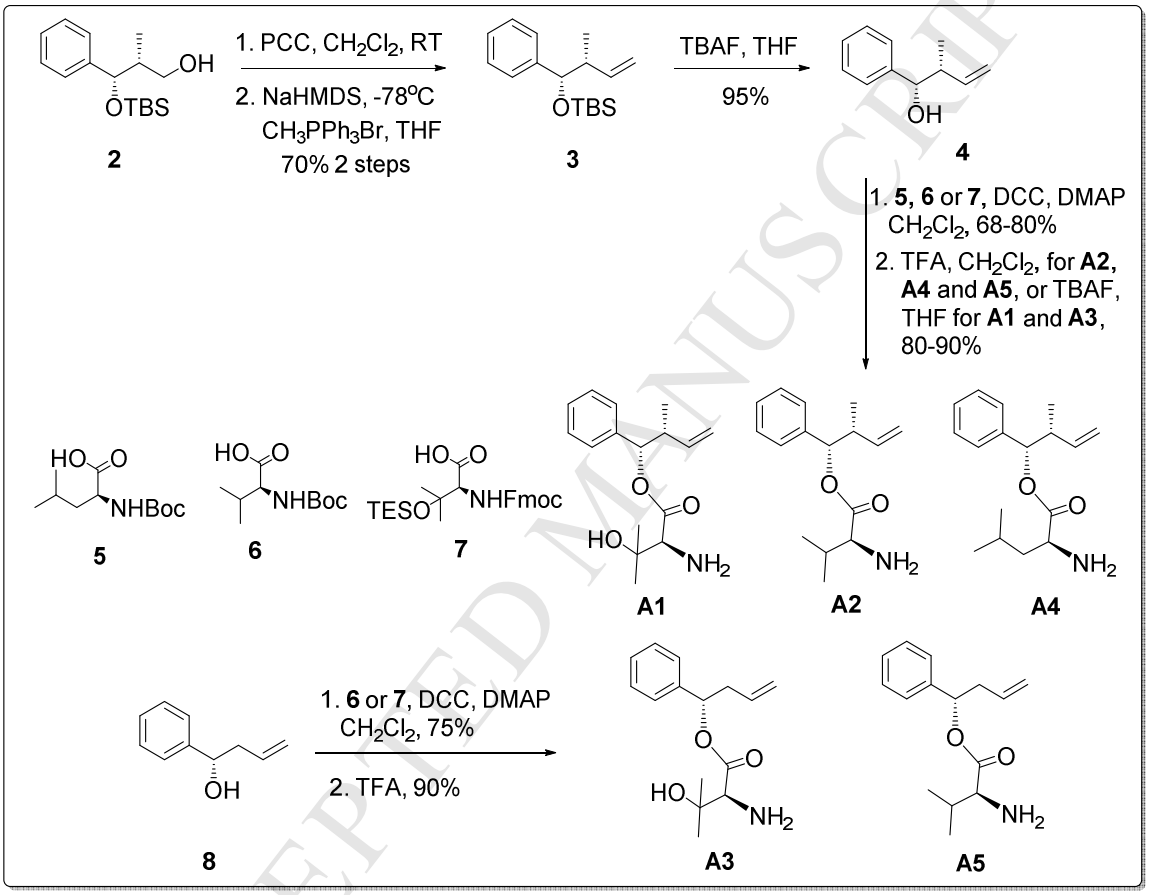


**Scheme 2** Synthesis of fragments **A1-5**

Fragment **B** was synthesized *via* a multiple step reaction as outlined in **Scheme 3**. Acid **B1** was prepared from aldehyde **9** [27]. Oxidation of allylic alcohol **11** gave rise to the corresponding carboxylic acid **B2** in a 90% yield [13]. Ester **12** could also be prepared from **9** by the protocol we used in the total synthesis of aetheramides [28]. Subsequent hydrolysis of ethyl ester **12** in the presence of lithium hydroxide in THF/$H_2O$ furnished the carboxylic acid **B3** in 86% yield. Alcohol **13** was synthesized according to the Kobayashi' protocol [29] from aldehyde **10** [30]. Methylation with Meerwein's salt ($Me_3OBF_4$) and proton sponge proceeded successfully to give the corresponding ether in 80% yield, and subsequent removal of Evans chiral auxiliary provided acid **B4** in 85% yield.

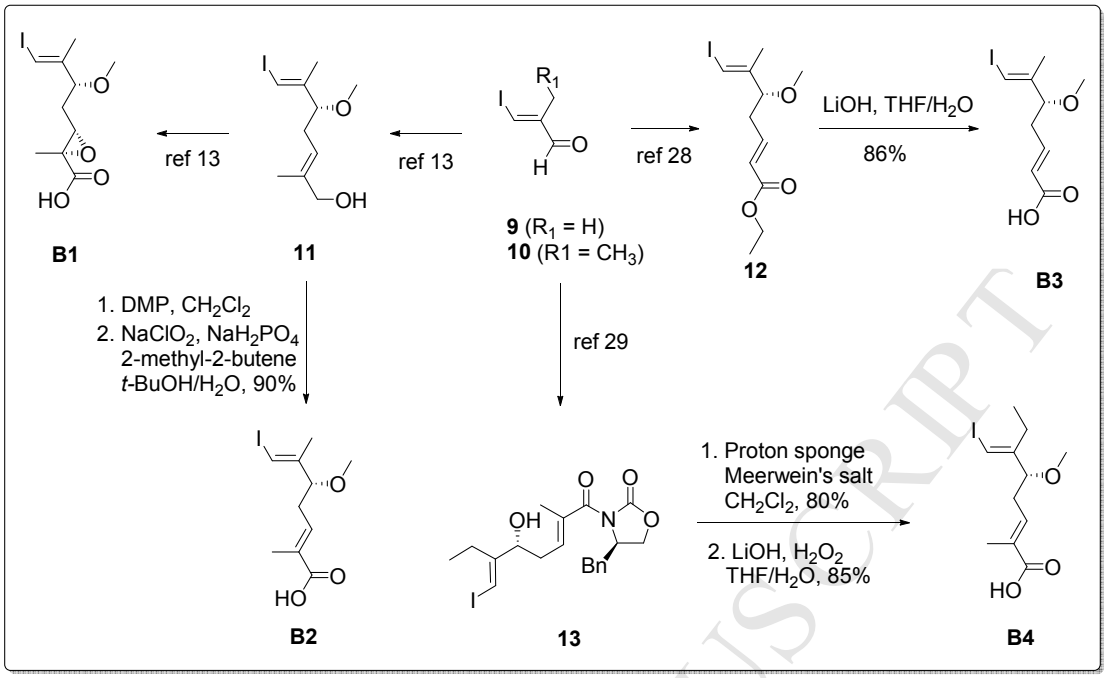


**Scheme 3.** Synthesis of fragments **B1-4**

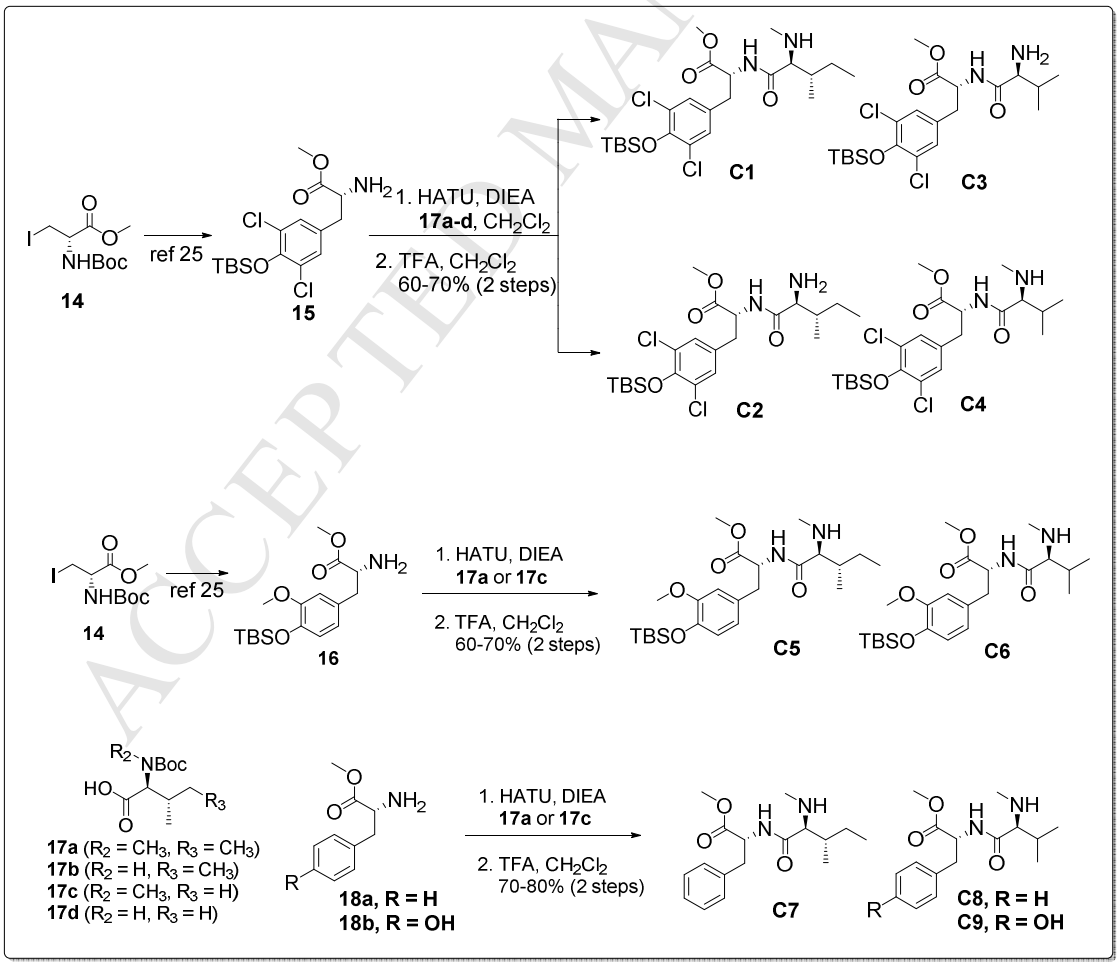


**Scheme 4.** Synthesis of fragments **C1-9**

The synthesis of fragment **C** started by preparing amines **15**, **16** and **18**. Amino esters **15** and **16** were prepared from β-iodo-D-alanine ester **14** by the Negishi reaction (**Scheme 4**) [28]. With precursors **15**, **16** and **18** in hand, fragment **C** was built *via* a two-step sequence. First, condensation of amines **15**, **16** and **18** with amino acids **17a-d** under the condition of HATU/DIPEA proceeded smoothly to afford the corresponding amides, which were treated with TFA to remove of Boc group, yielding amines **C1-9** in 60-80% yields.

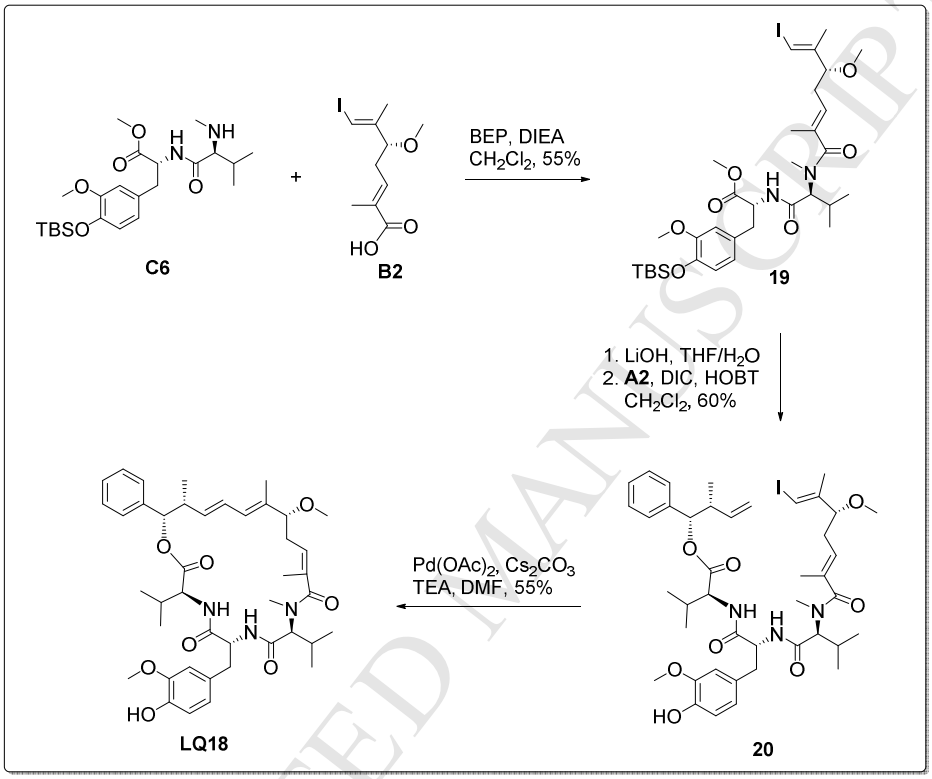


**Scheme 5** Synthesis of analogue **LQ18**

The synthesis of nannocystin A analogue **LQ18** is shown in **Scheme 5**. Amine **C6** and acid **B2** were coupled under standard condensation conditions to produce the amide **19** in 55% yield. Hydrolysis of methyl ester **19** with lithium hydroxide furnished the corresponding carboxylic acid, which was coupled with amine fragment **A2** using HATU/DIPEA to furnish iodide **20** directly. Finally, analogue **LQ18** was prepared by the intramolecular Heck reaction in 55% yield [15]. A series of nannocystin A analogues were prepared following the same procedure as for **LQ18** and their structures are listed in **Table 2**. All nannocystin A analogues were characterized by $^{1}$H NMR, $^{13}$C NMR and HRMS spectra (see Supporting Information).

**Table 2** Structures of nannocystin A analogues

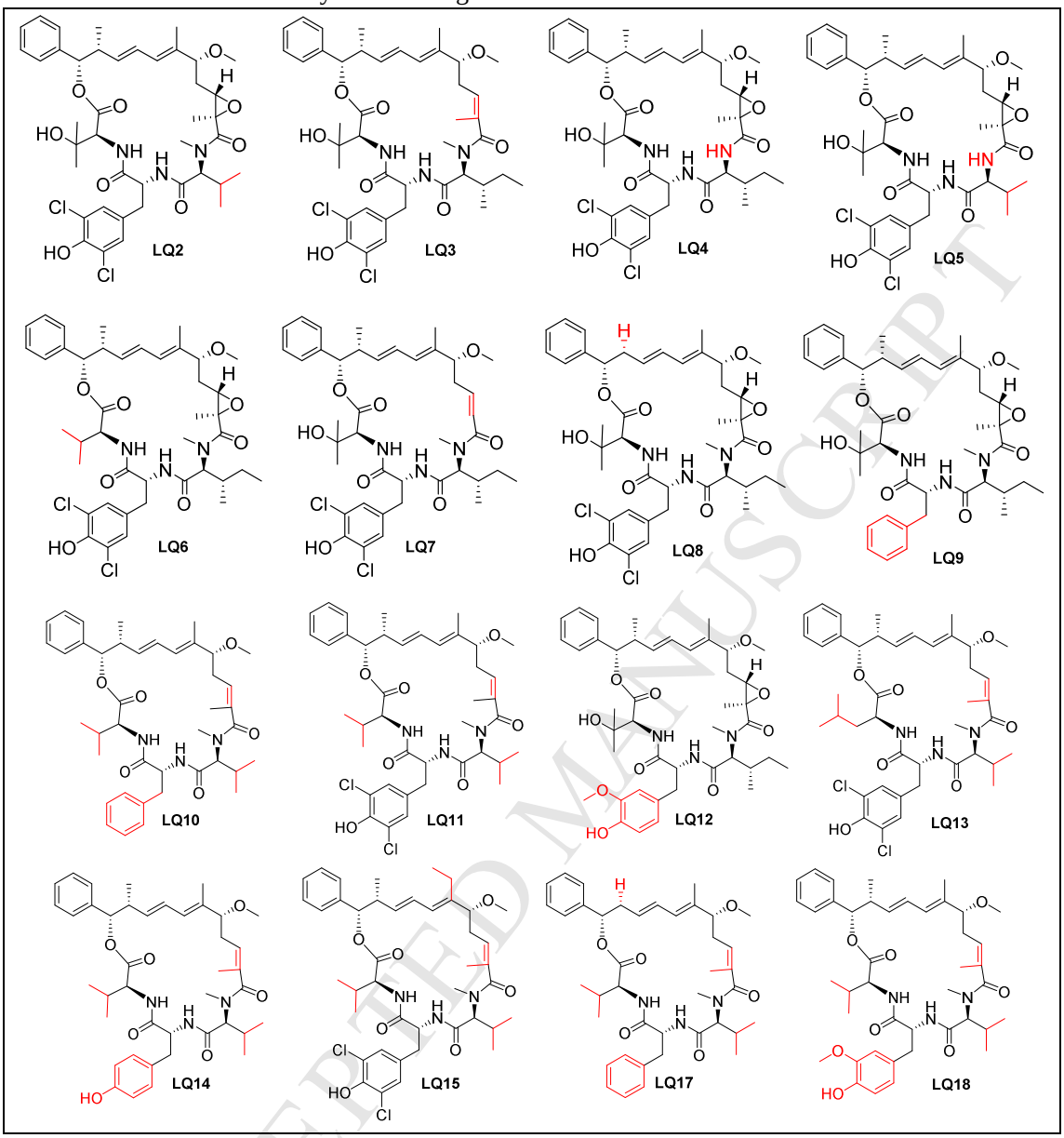


2.2 **SAR studies**

All nannocystin A analogues (**LQ2-18**) were evaluated for their antiproliferative activities on A549 and HCT-116 cell lines, and some of them were tested for their effects on the expression of the presumed target eEF1A1. The results of these biological evaluations were summarized in **Table 3** and **Fig. 2**.

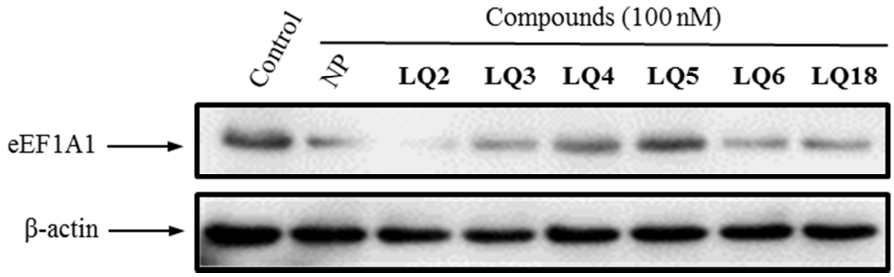


**Fig. 2** The protein expression of eEF1A1 in A549 cells after treatment with nannocystin A and analogues **LQ2-6** and **LQ18** was analyzed by Western blotting experiment. NP represents natural product nannocystin A.

As shown in **Tables 2** and **3**, the replacement of the *sec*-butyl group in nannocystin A by a isopropyl moiety (**LQ2**), or removal of a hydroxyl group from the isopropyl group in nannocystin A (**LQ6**) led to 2 or 3-fold increases in antiproliferative activity on both A549 and HCT-116 cell lines, while the removal of the (2*R*,3*S*)-epoxide in nannocystin A retained the anticancer activity for **LQ3** ($IC_{50}$ = 10.1 nM against A549), which is in consistence with the previously report [6], suggesting that the epoxide group is not involved in critical compound–protein interactions and could be removed. Further the methyl group removal from the unsaturated lactam in **LQ3** gave **LQ7**, which displayed a decreased anticancer activity ($IC_{50}$ = 40.5 nM against A549), suggesting that the methyl group is important and should be retained for good activity. Removal of *N*-methyl group in nannocystin A afforded **LQ4** and **LQ5**, which demolished all activities on the tested cell lines, indicating that the *N*-methyl is critical for its potency. In line with this observation, **LQ2** completely inhibited the expression of eEF1A1, while **LQ5** displayed little or no effect inhibiting its expression (**Fig. 2**). Removal of the methyl group at C-2 of nannocystin A (**LQ8**) led to a dramatic drop of anticancer activity, and deletion of all substitutes on benzyl moiety (**LQ9**) or the chlorine atom (**LQ12**) from nannocystin A maintained their anticancer potency. Examination of the docking model pose [6] suggested that a sub-pocket domain was near A375 of eEF1A which could accommodate the dimethyl group of nannocystin A. Replacement the dimethyl group at C-19 moiety of **LQ11** with a larger isopropyl group (**LQ13**) led to loss of potency, which could be explained by the collision of a bulkier side chain with the pocket. With these SAR information in hand, we incorporated all preferential modifications into nannocystin (**LQ10**) with the aim to further simplify its structure and improve potencies. To our disappointment, **LQ10** was ineffective on both cell lines. Finally, we optimized the substitutes on benzyl moiety of **LQ10**. A hydroxyl group was incorporated onto the benzyl group yield **LQ14**, which strongly inhibited A549 cell growth with an $IC_{50}$ value of 35.9 nM. Incorporation a methoxy group into the benzyl group of **LQ14** generated **LQ18** ($IC_{50}$ = 20.2 nM against A549), which displayed a comparable antiproliferative activity as nannocystin A. **LQ18** exhibited the same level of anticancer activity as

compared with nannocystin A, while it has a simplified chemical structure. Thus, we further explored its biologicals impact on other cell lines.

**Table 3** Antiproliferative activities of nannocystin A and its analogues **LQ2-18**

| Compounds | $IC_{50}$ (nM) [a] | |
|---|---|---|
| | A549 | HCT-116 |
| Nannocystin A | 13.1 ± 0.3 | 17 ± 2.0 |
| **LQ2** | 3.5 ± 1.1 | 6.7 ± 1.1 |
| **LQ3** | 10.1 ± 2.5 | 16.7 ± 1.3 |
| **LQ4** | 557 ± 116 | > 1000 |
| **LQ5** | NI | NI |
| **LQ6** | 3.2 ± 0.9 | 10.5 ± 2.2 |
| **LQ7** | 40.5 ± 10.1 | 123.8 ± 27.2 |
| **LQ8** | 90.3 ± 1.5 | 78.2 ± 9.4 |
| **LQ9** | 14.3 ± 0.6 | 20.9 ± 4.1 |
| **LQ10** | > 100 | > 100 |
| **LQ11** | 21.6 ± 3.4 | 42.1 ± 11.2 |
| **LQ12** | 3.7 ± 0.71 | 25.2 ± 2.6 |
| **LQ13** | > 100 | > 100 |
| **LQ14** | 35.9 ± 2.9 | 59.7 ± 8.8 |
| **LQ15** | 13.1 ± 3.6 | 60.3 ± 13.3 |
| **LQ17** | > 100 | > 100 |
| **LQ18** | 20.2 ± 2.9 | 48.5 ± 4.5 |
| **DOX** [b] | 459 ± 56 | 366 ± 43 |

[a] $IC_{50}$ values were calculated from three independent experiments by using the MTT assay after 72 h treatment. The values were reported as the Mean ± SD. [b] DOX represents doxorubicin, a positive control anticancer drug.

Then the anticancer activity of nannocystin A and **LQ18** on other cancer cell line was measured. As shown in **Table 4**, **LQ18** displayed potent inhibitory effect on all tested cell lines, and the $IC_{50}$ values ranged from 4.3 to 15.0 nM, similar to those of nannocystin A.

**Table 4** Comparison of nannocystin A and **LQ18** on the growth of different cell lines ($IC_{50}$, nM) [a]

| Compounds | $IC_{50}$ (nM) | | | |
|---|---|---|---|---|
| | MCF-7 | A375 | SH-SY-5Y | MDA-MB-231 |
| Nannocystin A | 8.7 ± 0.5 | 2.4 ± 0.29 | 2.1 ± 0.30 | 7.5 ± 0.30 |
| **LQ18** | 15.0 ± 3.2 | 4.3 ± 0.70 | 9.6 ± 0.6 | 12.5 ± 2.6 |

[a] $IC_{50}$ values were were reported as the Mean ± SD, which were derived from three independent experimental measurements.

2.3 **LQ18** inhibited A549 cell colony formation

The growth inhibitory effect of **LQ18** and nannocystin A against A549 was further measured by colony formation assay. As shown in **Fig. 3**, **LQ18** partially inhibited A549 cell colony formation at 5 nM, while it prevented its formation at 10 and 20 nM. As a comparison, nannocystin A at 10 nM was used to inhibited A549 colony formation, which also displayed potent inhibitory potency, as **LQ18** did at the same concentration. These results demonstrated that **LQ18** and nannocystin A have comparable anticancer activities.

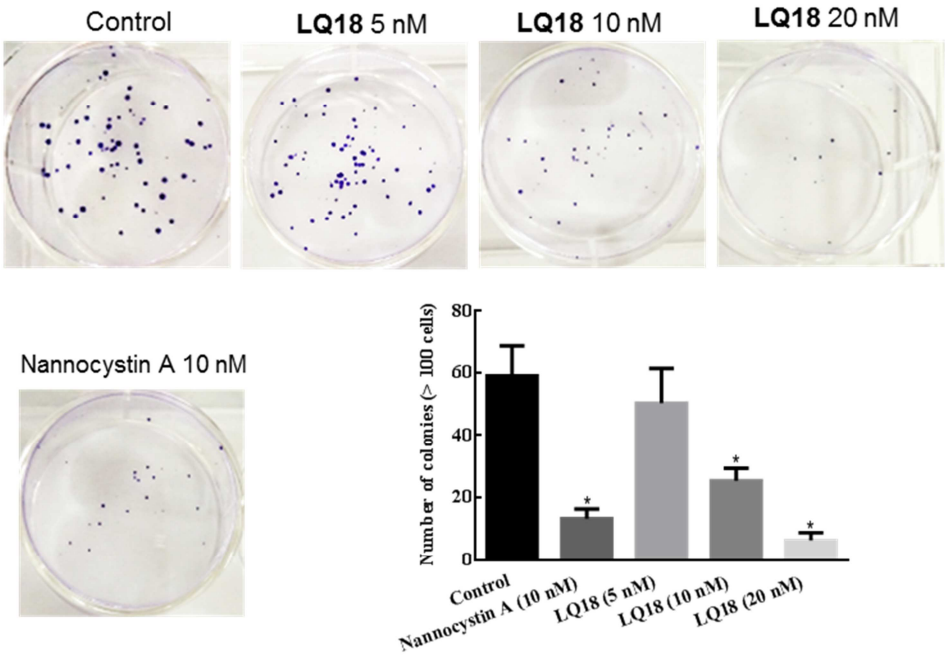


**Fig. 3 LQ18** inhibited A549 cell colonies formation. Bar chart representation of the colonies formed after **LQ18** treatment. One colony was defined to be an aggregate of over 100 cells. Nannocystin A was used as positive control. Data was shown as mean ± SD of three independent experiments. **P* < 0.05, versus control group.

2.4 **LQ18** arrested cell cycle at G2

Since **LQ18** showed the most promising anticancer potency, we conducted additional studies to investigate its biological roles in A549 cells. We examined the effect of **LQ18** on cell cycle distribution using the propidium iodide (PI) staining kit. A549 cells were treated with **LQ18** (30, 60, 90 nM), and nannocystin A (30 nM) or control for 24 h, then stained with PI and analyzed on a flow cytometer.

As shown in **Fig. 4**, **LQ18** led to a significant accumulation of cells at G2 phase from 30.02% to 37.66% (30 nM), 40.80% (60 nM) and 57.73% (90 nM), accordingly. At the same time, it reduced the cells at G1 phase from 57.41 to 37.81%, respectively. Meanwhile, we found that cell cycle arrest at G2 phase induced by **LQ18** was concentration-dependent, which might be one of

the possible mechanisms for its cytotoxicity.

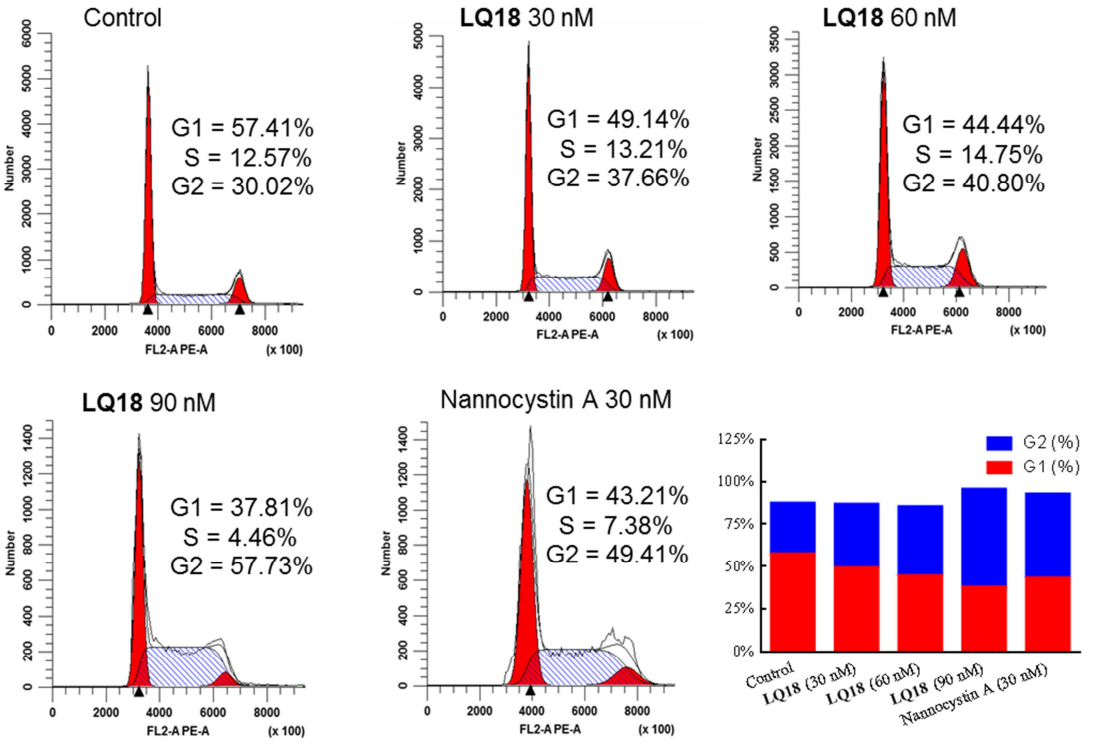


**Fig. 4 LQ18** induced cell cycle arrest in A549 cells. Cells were treated with **LQ18** for 30, 60, and 90 nM, and nannocystin A (30 nM) for 24 h, and then fixed in ice cold 70% ethanol at 4 °C, then stained with propidium iodide dye (50 µg/mL), and the cell cycle analysis was evaluated *via* flow cytometry (CytoFLEX, Beck- man, USA). The insert bar graph showed the percentages (%) of cells in G1 and G2 phases, respectively.

**2.5 LQ18** induced A549 cell apoptosis

To explore the mechanism of cells death, A549 cells were treated by **LQ18** (30, 60, and 90 nM) and nannocystin A (30 nM) for 12 h to induce cells apoptosis, which was then examined with Annexin V-FITC/PI FACS assay. As shown in **Fig. 5A**, the percentages of apoptotic population in A549 cells treated with **LQ18** (30, 60, and 90 nM) for 12 h were 14.81, 23.58 and 31.77%, respectively, suggesting that the induction of apoptosis in A549 cells follows a dose-dependent manner, while for nannocystin A at 30 nM, the percentage was 26.99%. To verify this observation, A549 cells were treated with **LQ18** for 24 h and then stained with Hoechst 33342 dye. The cells were then photographed by a confocal laser scanning microscopy. The A549 cells treated with higher concentrations of **LQ18** displayed stronger blue fluorescence (**Fig. 5B**), indicating an increase of apoptosis caused by higher concentrations of **LQ18**.

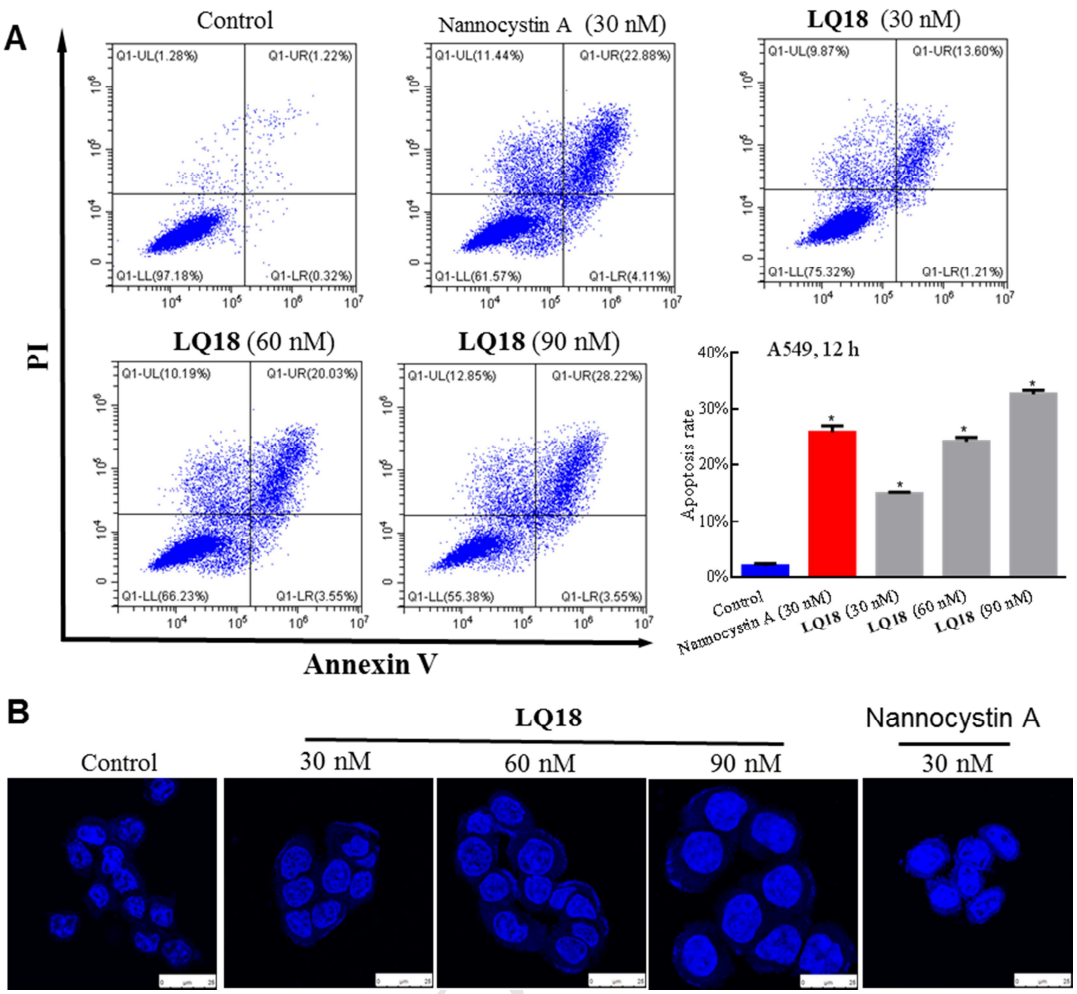


**Fig. 5 LQ18** induced A549 cells apoptosis. (A) A549 cells were treated with various concentrations of **LQ18** as indicated for 12 h, then cells were stained with annexin V / PI, and apoptosis was analyzed by using a flow cytometry. The insert bar graph represents statistics of total apoptotic cell percentages from duplicate experiments; (B) Confocal laser scanning microscopy analysis of nuclei fragmentation by Hoechst 33342 staining. Representative photomicrographs of A549 cell line stained with Hoechst 33342 fluorescent dye after exposure to **LQ18** (30, 60 and 90 nM) or nannocystin A (30 nM) for 24 h. The control group cells exhibited pale blue fluorescence, while the apoptotic cells exhibited strong blue fluorescence. Scale bars = 25 μm. *$P < 0.05$, versus control group.

Moreover, the percentages of apoptosis for A549 cells treated with **LQ18** in 60 nM for 6, 12, and 24 h were 5.42, 23.58, and 32.51%, respectively, suggesting that the induction of apoptosis in A549 cells by LQ18 was time-dependent (**Fig. 6A**). To explore the apoptosis mechanism of A549 cells caused by **LQ18**, we examined the expressions of caspase-3, caspase-9, bax and bcl-2 proteins after **LQ18** treatment (**Fig. 6B**). The expressions of caspase-3, caspase-9 and bax increased in a dose-dependent manner after **LQ18** treatment, whereas the bcl-2 expression was obviously decreased.

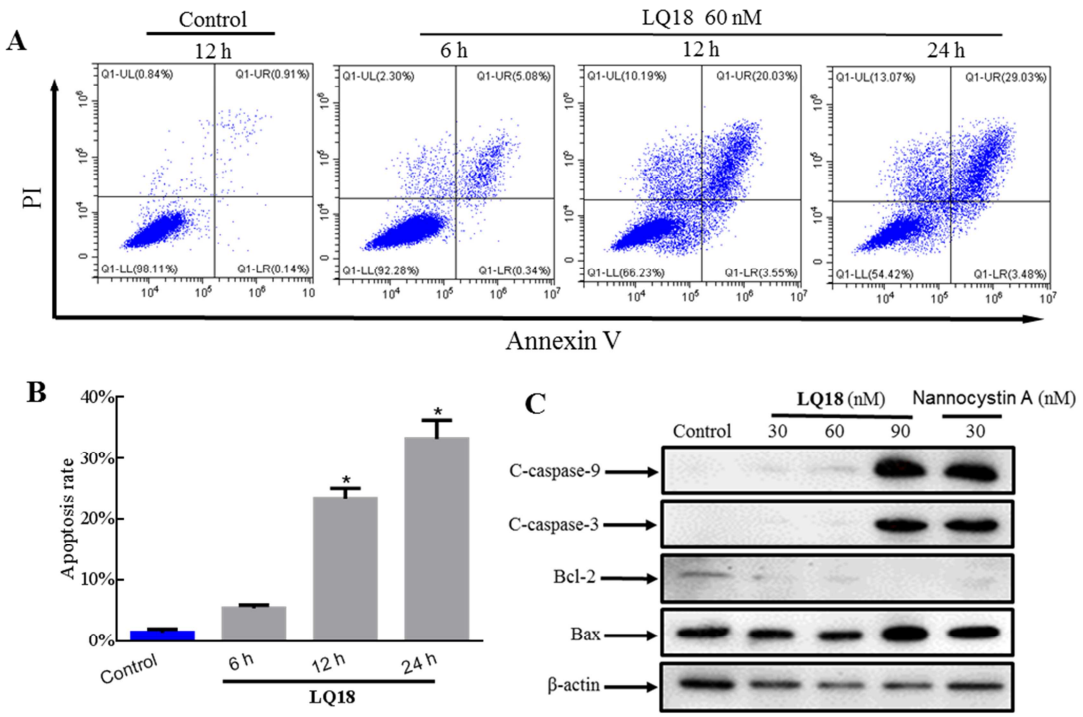


**Fig. 6 LQ18** induced A549 cells apoptosis. (A) A549 cells were treated with various **LQ18** at 60 nM for 6, 12 and 24 h, then cells were stained with Annexin V / PI, and apoptosis was analyzed by using a flow cytometry; (B) The bar graph represents statistics of total apoptotic cell percentages from duplicate experiments; (C) **LQ18** induced caspases activation, down-regulation of Bcl-2 and up-regulation of Bax in A549 cells. Cells were treated with various concentrations of **LQ18** as indicated for 24 h. *P < 0.05, versus control group.

### 3. Conclusion

We herein report the synthesis of a series of novel nannocystin A analogues and evaluation of their anticancer activities on A549 and HCT116 cells. The effects of some nannocystin A analogs on the eEF1A1 expression were also measured. Based on their antiproliferative activities against multiple cancer cell lines and ability to inhibit eEF1A1 protein expression, we identified a novel nannocystin A analogue **LQ18**, which exhibited potent antiproliferative activities with $IC_{50}$ values of 20.2, 4.3, and 9.6 nM against A549, A375, and SH-SY-5Y, respectively. **LQ18** exhibited a comparable anticancer activity as nannocystin A did, while it has a simplified chemical structure. Further biological evaluations suggested that **LQ18** arrested cell cycle at G2 phase and induce A549 cell apoptosis *via* up-regulation of caspase-3, caspase-9 and bax protein expressions in a dose-dependent manner, whereas the bcl-2 expression was significantly decreased. All these data demonstrated that **LQ18** could be a promising lead for the development of structurally novel eEF1A1 inhibitor for the treatment of cancers.

## 4. Experimental section

4.1 Materials and methods

All chemicals were purchased from commercial sources and used as received. For detailed materials information and methods, please see Supporting Information.

4.2 Chemicals synthesis of intermediates

All the synthetic procedures of intermediates were listed in Supporting Information.

4.3 Chemical synthesis and spectra data of the target compounds **LQ2-18**

*(3S,6R,9S,12E,15R,16E,18E,20R,21S)-6-(4-Hydroxy-3-methoxybenzyl)-3,9-diisopropyl-15-methoxy-10,12,16,20-tetramethyl-21-phenyl-1-oxa-4,7,10-triazacyclohenicosa-12,16,18-triene-2,5,8,11-tetraone (**LQ18**)*

To a solution of **20** (30 mg, 0.035 mmol, 1 equiv) in DMF (3 mL) was added $Pd(OAc)_2$ (8 mg, 0.035 mmol, 1 equiv), $Cs_2CO_3$ (23 mg, 0.070 mmol, 2 equiv) and TEA (5 mg, 0.053 mmol, 1.5 equiv). The reaction was stirred at room temperature for 2 h, diluted with EtOAc (5 mL) and $H_2O$ (5 mL), the mixtures were separated and the aqueous layer was extracted with EtOAc (5 mL × 3), the combined organic layers were washed with brine, dried over anhydrous $Na_2SO_4$, concentrated and purified with silica gel column chromatography (petroleum ether: EtOAc = 1:1) to afford compound **LQ18** (14 mg, 55%). $[\alpha]_D^{28}$ = -64 (*c* 0.2, $CHCl_3$); IR (KBr) $\nu_{max}$ 3564, 3520, 3482, 1644, 700, 665, 607 $cm^{-1}$; $^1H$ NMR (600 MHz, $CDCl_3$) $\delta$ 7.31 (t, *J* = 7.2 Hz, 2H), 7.27−7.24 (m, 4H), 7.22 (d, *J* = 7.8 Hz, 1H), 6.93 (d, *J* = 9.0 Hz, 1H), 6.78 (d, *J* = 8.4 Hz, 1H), 6.74 (s, 1H), 6.72 (d, *J* = 7.8 Hz, 1H), 6.53 (d, *J* = 9.0 Hz, 1H), 6.33−6.24 (m, 1H), 6.01 (s, 1H), 5.86 (d, *J* = 10.8 Hz, 1H), 5.77 (dd, *J* = 15.0, 4.8 Hz, 1H), 5.50 (s, 1H), 5.43 (t, *J* = 7.2 Hz, 1H), 4.61 (dd, *J* = 9.0, 3.6 Hz, 1H), 4.58−4.53 (m, 1H), 4.51 (d, *J* = 10.5 Hz, 1H), 3.84 (s, 3H), 3.55 (dd, *J* = 10.8, 3.0 Hz, 1H), 3.19 (s, 3H), 3.01 (dd, *J* = 13.8, 9.6 Hz, 1H), 2.86 (dd, *J* = 13.2, 5.4 Hz, 1H), 2.69 (s, 3H), 2.63−2.52 (m, 2H), 2.41−2.35 (m, 1H), 2.35−2.29 (m, 1H), 2.24−2.19 (m, 1H), 1.81 (s, 3H), 1.75 (s, 3H), 1.03 (d, *J* = 6.6 Hz, 3H), 0.95 (d, *J* = 6.6 Hz, 3H), 0.86 (d, *J* = 6.6 Hz, 3H), 0.67 (d, *J* = 6.6 Hz, 3H), 0.47 (d, *J* = 6.6 Hz, 3H); $^{13}C$ NMR (150 MHz, $CDCl_3$) $\delta$ 175.5 (C=O), 170.8 (C=O), 170.5 (C=O), 170.5 (C=O), 146.4, 144.4, 139.2, 136.3, 135.1, 133.4, 128.7, 128.4, 128.2, 127.7, 127.6, 125.8, 125.5, 122.1, 114.3, 111.7, 85.9, 78.0, 61.7, 56.0, 55.9, 55.8, 54.8, 42.3, 36.6, 32.2, 31.8, 31.4, 29.3, 24.9, 19.9, 19.0, 18.4, 16.2, 14.4, 11.1, 9.8.; HRMS (ESI): calcd for $C_{42}H_{57}N_3O_0Na^+$ [M+$Na^+$] 754.4038, found 754.4030.

*(1R,4S,7R,10S,13S,14R,15E,17E,19R,21S)-7-(3,5-Dichloro-4-hydroxybenzyl)-10-(2-hydroxypropan-2-yl)-4-isopropyl-19-methoxy-1,3,14,18-tetramethyl-13-phenyl-12,22-dioxa-3,6,9-triazabicyclo[19.1.0]docosa-15,17-diene-2,5,8,11-tetraone (**LQ2**)*

**LQ2** was obtained following the procedure for **LQ18** in 53% yield. $[\alpha]_D^{28}$ = -17.5 (*c* 0.08, $CHCl_3$); IR (KBr) $\nu_{max}$ 3447, 3416, 1639, 1619, 762, 619 $cm^{-1}$; $^1H$ NMR (600 MHz, $CDCl_3$) $\delta$

7.44−7.29 (m, 5H), 7.07 (s, 2H), 6.60 (d, *J* = 6.6 Hz, 1H), 6.46 (d, *J* = 7.8 Hz, 1H), 6.33 (dd, *J* = 15.0, 10.8 Hz, 1H), 6.15 (d, *J* = 10.8 Hz, 1H), 5.93 (d, *J* = 2.4 Hz, 1H), 5.85 (dd, *J* = 15.0, 5.4 Hz, 1H), 4.62 (q, *J* = 7.2 Hz, 1H), 4.58 (d, *J* = 7.8 Hz, 1H), 4.39 (d, *J* = 11.4 Hz, 1H), 3.69 (dd, *J* = 9.0, 2.4 Hz, 1H), 3.20 (s, 3H), 3.13 (s, 3H), 3.07 (dd, *J* = 8.4, 3.6 Hz, 1H), 2.94 (dd, *J* = 14.4, 7.2 Hz, 1H), 2.76−2.68 (m, 1H), 2.63 (dd, *J* = 13.8, 6.6 Hz, 1H), 2.35−2.25 (m, 2H), 2.09−2.02 (m, 1H), 1.73 (s, 3H), 1.53 (s, 3H), 1.20 (s, 3H), 1.17 (s, 3H), 1.05 (d, *J* = 6.6 Hz, 3H), 0.86 (d, *J* = 6.6 Hz, 3H), 0.79 (d, *J* = 6.6 Hz, 3H); $^{13}$C NMR (150 MHz, $CDCl_3$) *δ* 171.0 (C=O), 170.2 (C=O), 169.5 (C=O), 169.0 (C=O), 146.8, 138.0, 135.7, 134.1, 129.6, 129.1, 128.3, 128.1, 126.8, 126.4, 126.3, 121.0, 83.9, 82.1, 80.3, 72.1, 65.5, 62.5, 61.8, 60.6, 59.9, 58.6, 56.6, 56.1, 54.9, 53.9, 42.3, 41.8, 37.7, 31.5, 29.8, 29.7, 27.0, 26.5, 25.7, 19.2, 18.4, 15.6, 11.8; HRMS (ESI): calcd for $C_{41}H_{53}Cl_2N_3O_9Na^+$ [M+$Na^+$] 824.3051, found 824.3061.

*(3S,6R,9S,12E,15R,16E,18E,20R,21S)-9-((S)-Sec-butyl)-6-(3,5-dichloro-4-hydroxybenzyl)-3-(2-hydroxypropan-2-yl)-15-methoxy-10,12,16,20-tetramethyl-21-phenyl-1-oxa-4,7,10-triazacyclohenicosa-12,16,18-triene-2,5,8,11-tetraone (**LQ3**)*

**LQ3** was obtained following the procedure for **LQ18** in 50% yield. $[\alpha]_D^{28}$ = -62.5 (*c* 0.08, $CHCl_3$); $^1$H NMR (600 MHz, $CDCl_3$) *δ* 7.38−7.29 (m, 5H), 7.02 (s, 2H), 6.41 (d, *J* = 6.6 Hz, 1H), 6.32 (dd, *J* = 15.0, 11.4 Hz, 1H), 5.86 (s, 1H), 5.85 (d, *J* = 9.6 Hz, 1H), 5.72 (s, 1H), 5.54 (dd, *J* = 15.0, 6.6 Hz, 1H), 5.47 (t, *J* = 7.2 Hz, 1H), 4.63 (q, *J* = 8.4 Hz, 1H), 4.57 (d, *J* = 9.0 Hz, 1H), 4.33 (d, *J* = 10.8 Hz, 1H), 3.66 (dd, *J* = 7.8, 3.0 Hz, 1H), 3.23 (s, 3H), 2.95 (dd, *J* = 13.8, 7.2 Hz, 1H), 2.82 (s, 3H), 2.81−2.77 (m, 1H), 2.73 (dd, *J* = 14.4, 6.6 Hz, 1H), 2.55−2.47 (m, 1H), 2.46−2.38 (m, 1H), 2.13−2.04 (m, 1H), 1.80 (s, 3H), 1.71 (s, 3H), 1.48−1.40 (m, 1H), 1.05 (s, 3H), 1.04 (d, *J* = 8.4 Hz, 3H), 0.94 (t, *J* = 7.2 Hz, 3H), 0.85 (d, *J* = 6.0 Hz, 3H); $^{13}$C NMR (150 MHz, $CDCl_3$) *δ* 176.2 (C=O), 170.8 (C=O), 170.1 (C=O), 169.2 (C=O), 146.7, 137.7, 134.6, 134.3, 133.2, 129.7, 129.0, 127.9, 127.8, 127.1, 126.9, 126.7, 121.0, 84.8, 80.4, 72.2, 61.8, 60.7, 56.3, 53.7, 41.7, 35.9, 32.6, 31.4, 31.2, 29.7, 26.9, 26.6, 25.4, 15.9, 14.3, 13.0, 12.8, 10.6.

*(1R,4S,7R,10S,13S,14R,15E,17E,19R,21S)-4-((S)-Sec-butyl)-7-(3,5-dichloro-4-hydroxybenzyl)-10-(2-hydroxypropan-2-yl)-19-methoxy-1,14,18-trimethyl-13-phenyl-12,22-dioxa-3,6,9-triazabicyclo[19.1.0]docosa-15,17-diene-2,5,8,11-tetraone (**LQ4**)*

**LQ4** was obtained following the procedure for **LQ18** in 58% yield. $[\alpha]_D^{28}$ = 12 (*c* 0.1, $CHCl_3$); IR (KBr) $\nu_{max}$ 3512, 3447, 1649, 1632, 684 $cm^{-1}$; $^1$H NMR (600 MHz, $CDCl_3$) *δ* 7.44−7.23 (m, 5H), 7.22−7.13 (m, 1H), 7.09 (s, 2H), 6.98 (d, *J* = 8.0 Hz, 1H), 6.76 (d, *J* = 9.2 Hz, 1H), 6.40−6.25 (m, 2H), 6.13−6.01 (m, 2H), 5.98 (s, 1H), 5.77 (dd, *J* = 15.2, 7.6 Hz, 1H), 4.73 (q, *J* = 7.6 Hz, 1H), 4.50 (d, *J* = 8.0 Hz, 1H), 4.21 (dd, *J* = 8.8, 6.4 Hz, 1H), 3.74 (d, *J* = 5.6 Hz, 1H), 3.22 (s, 3H), 2.97 (dd, *J* = 14.4, 6.8 Hz, 1H), 2.84 (d, *J* = 5.6 Hz, 1H), 2.82−2.72 (m, 2H), 2.72−2.63 (m, 1H), 2.00−1.95 (m, 1H), 1.90−1.77 (m, 2H), 1.69 (s, 3H), 1.50 (s, 3H), 1.22 (s, 3H), 1.13 (s, 3H), 1.00 (d, *J* = 6.8 Hz, 3H), 0.82 (t, *J* = 7.2 Hz, 3H), 0.77 (d, *J* = 6.4 Hz, 3H); $^{13}$C NMR (150 MHz, $CDCl_3$)

$\delta$ 171.4 (C=O), 170.9 (C=O), 170.3 (C=O), 170.1 (C=O), 147.0, 137.8, 135.8, 133.9, 129.5, 128.9, 128.2, 128.0, 127.2, 126.8, 126.4, 121.3, 83.1, 80.0, 71.5, 60.6, 60.2, 60.1, 57.2, 56.3, 53.8, 42.6, 37.2, 36.9, 31.4, 29.7, 27.0, 26.5, 24.7, 15.2, 13.7, 13.0, 12.5, 11.4; HRMS (ESI): calcd for $C_{41}H_{53}Cl_2N_3O_9Na^+$ [M+$Na^+$] 824.3051, found 824.3057.

*(1R,4S,7R,10S,13S,14R,15E,17E,19R,21S)-7-(3,5-Dichloro-4-hydroxybenzyl)-10-(2-hydroxypropa n-2-yl)-4-isopropyl-19-methoxy-1,14,18-trimethyl-13-phenyl-12,22-dioxa-3,6,9-triazabicyclo[19.1 .0]docosa-15,17-diene-2,5,8,11-tetraone (**LQ5**)*

**LQ5** was obtained following the procedure for **LQ18** in 58% yield. $[\alpha]_D^{28}$ = 20 (*c* 0.15, $CHCl_3$); IR (KBr) $\nu_{max}$ 3511, 3445, 1627, 1652, 1285, 770 $cm^{-1}$; $^1$H NMR (600 MHz, $CDCl_3$) $\delta$ 7.38−7.25 (m, 5H), 7.10 (s, 2H), 6.76 (d, *J* = 9.0 Hz, 1H), 6.61 (d, *J* = 7.8 Hz, 1H), 6.46−6.35 (m, 1H), 6.31 (dd, *J* = 15.0, 10.8 Hz, 1H), 6.06 (d, *J* = 10.8 Hz, 1H), 6.00 (s, 1H), 5.78 (dd, *J* = 15.0, 7.2 Hz, 1H), 4.77 (q, *J* = 7.8 Hz, 1H), 4.55 (d, *J* = 8.4 Hz, 1H), 4.18 (dd, *J* = 9.0, 6.0 Hz, 1H), 3.74 (dd, *J* = 9.0, 3.0 Hz, 1H), 3.20 (s, 3H), 3.18−3.14 (m, 1H), 2.95 (dd, *J* = 13.8, 6.6 Hz, 1H), 2.84 (t, *J* = 6.0 Hz, 1H), 2.79 (dd, *J* = 14.4, 7.8 Hz, 1H), 2.71−2.64 (m, 1H), 2.05−1.95 (m, 2H), 1.93−1.86 (m, 1H), 1.85−1.78 (m, 1H), 1.67 (s, 3H), 1.49 (s, 3H), 1.21 (s, 3H), 1.11 (s, 3H), 0.99 (d, *J* = 6.6 Hz, 3H), 0.80 (d, *J* = 6.6 Hz, 3H), 0.76 (d, *J* = 7.2 Hz, 3H); $^{13}$C NMR (150 MHz, $CDCl_3$) $\delta$ 171.5 (C=O), 170.8 (C=O), 170.5 (C=O), 170.2 (C=O), 147.1, 138.0, 135.9, 133.8, 129.5, 129.0, 128.2, 127.9, 127.8, 126.6, 126.3, 121.4, 83.3, 79.8, 71.7, 60.4, 60.1, 60.1, 57.7, 56.2, 53.8, 42.6, 37.2, 31.5, 30.9, 29.7, 26.8, 26.4, 19.0, 17.5, 13.6, 12.7, 12.0; HRMS (ESI): calcd for $C_{40}H_{51}Cl_2N_3O_9Na^+$ [M+$Na^+$] 810.2895, found 810.2891.

*(1R,4S,7R,10S,13S,14R,15E,17E,19R,21S)-4-((S)-Sec-butyl)-7-(3,5-dichloro-4-hydroxybenzyl)-10-isopropyl-19-methoxy-1,3,14,18-tetramethyl-13-phenyl-12,22-dioxa-3,6,9-triazabicyclo[19.1.0]do cosa-15,17-diene-2,5,8,11-tetraone (**LQ6**)*

**LQ6** was obtained following the procedure for **LQ18** in 56% yield. $[\alpha]_D^{28}$ = -39 (*c* 0.2, $CHCl_3$); IR (KBr) $\nu_{max}$ 3466, 3425, 1627, 1590, 1248, 740 $cm^{-1}$; $^1$H NMR (600 MHz, $CDCl_3$) $\delta$ 7.38−7.18 (m, 5H), 7.12 (s, 2H), 6.89 (d, *J* = 7.2 Hz, 1H), 6.37−6.27 (m, 1H), 6.12 (s, 1H), 6.09 (d, *J* = 10.8 Hz, 1H), 6.06−6.00 (m, 1H), 6.01 (d, *J* = 8.4 Hz, 1H), 5.88 (dd, *J* = 15.0, 4.2 Hz, 1H), 4.71 (dd, *J* = 8.4, 3.0 Hz, 1H), 4.54 (q, *J* = 6.0 Hz, 1H), 4.50 (d, *J* = 11.4 Hz, 1H), 3.65 (dd, *J* = 10.8, 2.4 Hz, 1H), 3.16 (s, 3H), 3.08 (s, 3H), 2.96−2.80 (m, 3H), 2.69−2.61 (m, 1H), 2.27−2.07 (m, 3H), 1.94−1.84 (m, 1H), 1.75 (s, 3H), 1.55−1.46 (m, 1H), 1.51 (s, 3H), 1.36−1.29 (m, 1H), 1.03 (d, *J* = 7.2 Hz, 3H), 1.02−0.96 (m, 1H), 0.88 (t, *J* = 4.2 Hz, 3H), 0.84 (d, *J* = 3.0 Hz, 3H), 0.83 (d, *J* = 2.4 Hz, 3H), 0.60 (d, *J* = 7.2 Hz, 3H); $^{13}$C NMR (150 MHz, $CDCl_3$) $\delta$ 170.9 (C=O), 170.7 (C=O), 169.8 (C=O), 168.5 (C=O), 147.0, 139.0, 136.3, 134.0, 129.7, 129.7, 129.1, 128.3, 127.7, 125.8, 125.7, 121.1, 84.7, 78.5, 61.6, 60.5, 58.5, 56.4, 55.6, 54.4, 42.1, 38.7, 31.7, 31.1, 29.8, 24.3, 19.0, 16.4, 15.5, 15.4, 10.7, 10.4, 9.5; HRMS (ESI): calcd for $C_{42}H_{55}Cl_2N_3O_8Na^+$ [M+$Na^+$] 822.3258, found 822.3263.

*(3S,6R,9S,12E,15R,16E,18E,20R,21S)-9-((S)-Sec-butyl)-6-(3,5-dichloro-4-hydroxybenzyl)-3-(2-hydroxypropan-2-yl)-15-methoxy-10,16,20-trimethyl-21-phenyl-1-oxa-4,7,10-triazacyclohenicosa-12,16,18-triene-2,5,8,11-tetraone (**LQ7**)*

**LQ7** was obtained following the procedure for **LQ18** in 60% yield. $[\alpha]_D^{28}$ = -50 (*c* 0.15, $CHCl_3$); IR (KBr) $\nu_{max}$ 3693, 3401, 1724, 1659, 1201, 761 $cm^{-1}$; $^1H$ NMR (600 MHz, $CDCl_3$) $\delta$ 7.48 (t, *J* = 7.8 Hz, 2H), 7.48 (t, *J* = 7.2 Hz, 1H), 7.31 (d, *J* = 7.2 Hz, 2H), 6.90 (s, 2H), 6.82−6.73 (m, 1H), 6.26 (dd, *J* = 15.0, 10.8 Hz, 1H), 6.20−6.12 (m, 2H), 6.03 (d, *J* = 11.4 Hz, 1H), 5.80 (d, *J* = 3.6 Hz, 1H), 5.82−5.75 (m, 1H), 5.51 (dd, *J* = 15.0, 9.0 Hz, 1H), 4.63−4.54 (m, 2H), 4.32 (d, *J* = 8.4 Hz, 1H), 3.76−3.69 (m, 1H), 3.28 (s, 3H), 2.98 (s, 3H), 2.84−2.76 (m, 1H), 2.74−2.66 (m, 1H), 2.45−2.36 (m, 1H), 2.07 (s, 1H), 2.04−1.95 (m, 1H), 1.84−1.74 (m, 1H), 1.68 (s, 3H), 1.68−1.62 (m, 3H), 1.33 (s, 3H), 1.17 (s, 3H), 0.99 (d, *J* = 7.2 Hz, 3H), 0.97−0.92 (m, 1H), 0.85 (t, *J* = 7.2 Hz, 3H), 0.64 (d, *J* = 6.0 Hz, 3H); $^{13}C$ NMR (150 MHz, $CDCl_3$) $\delta$ 170.6 (C=O), 170.4 (C=O), 168.7 (C=O), 168.1 (C=O), 146.6, 141.5, 136.3, 134.4, 133.7, 130.2, 128.5, 128.4, 128.2, 128.0, 126.8, 125.0, 122.8, 120.9, 83.4, 80.4, 70.7, 61.5, 60.9, 56.5, 53.3, 41.9, 35.6, 35.4, 31.6, 30.6, 29.7, 27.3, 27.0, 24.5, 15.3, 15.2, 14.4, 10.5; HRMS (ESI): calcd for $C_{41}H_{53}Cl_2N_3O_8Na^+$ [M+$Na^+$] 808.3102, found 808.3121.

*(1R,4S,7R,10S,13S,15E,17E,19R,21S)-4-((S)-Sec-butyl)-7-(3,5-dichloro-4-hydroxybenzyl)-10-(2-hydroxypropan-2-yl)-19-methoxy-1,3,18-trimethyl-13-phenyl-12,22-dioxa-3,6,9-triazabicyclo[19.1.0]docosa-15,17-diene-2,5,8,11-tetraone (**LQ8**)*

**LQ8** was obtained following the procedure for **LQ18** in 60% yield. $[\alpha]_D^{28}$ = -24 (*c* 0.1, $CHCl_3$); IR (KBr) $\nu_{max}$ 3618, 3534, 3334, 1737, 1664, 1384, 965, 743 $cm^{-1}$; $^1H$ NMR (600 MHz, $CDCl_3$) $\delta$ 7.47−7.29 (m, 5H), 7.17 (s, 2H), 6.89 (d, *J* = 6.6 Hz, 1H), 6.47−6.38 (m, 1H), 6.22 (d, *J* = 8.4 Hz, 1H), 6.07 (d, *J* = 10.8 Hz, 1H), 5.90 (d, *J* = 11.4 Hz, 1H), 5.82 (s, 1H), 5.71−5.62 (m, 1H), 4.64−4.52 (m, 2H), 4.49 (d, *J* = 11.4 Hz, 1H), 3.66 (dd, *J* = 11.4, 3.0 Hz, 1H), 3.17 (s, 3H), 3.09 (s, 3H), 2.98−2.91 (m, 2H), 2.91−2.81 (m, 2H), 2.58 (d, *J* = 10.8 Hz, 1H), 2.20−2.07 (m, 2H), 2.06−1.97 (m, 2H), 1.76 (s, 3H), 1.55−1.49 (m, 1H), 1.51 (s, 3H), 1.34−1.31 (m, 1H), 1.04−0.99 (m, 1H), 1.02 (s, 3H), 0.89 (t, *J* = 7.2 Hz, 3H), 0.82 (d, *J* = 6.6 Hz, 3H), 0.80 (s, 3H); $^{13}C$ NMR (150 MHz, $CDCl_3$) $\delta$ 170.7 (C=O), 170.2 (C=O), 170.1 (C=O), 168.6 (C=O), 146.9, 139.1, 134.5, 129.8, 129.5, 129.4, 129.3, 129.2, 128.9, 128.7, 127.1, 121.0, 84.8, 72.9, 61.7, 60.5, 59.8, 58.6, 55.7, 54.2, 39.8, 38.6, 31.7, 31.2, 29.8, 29.7, 27.2, 25.4, 24.3, 15.5, 15.4, 10.5, 10.4.; HRMS (ESI): calcd for $C_{41}H_{53}Cl_2N_3O_9Na^+$ [M+$Na^+$] 824.3051, found 824.3057.

*(1R,4S,7R,10S,13S,14R,15E,17E,19R,21S)-7-Benzyl-4-((S)-sec-butyl)-10-(2-hydroxypropan-2-yl)-19-methoxy-1,3,14,18-tetramethyl-13-phenyl-12,22-dioxa-3,6,9-triazabicyclo[19.1.0]docosa-15,17-diene-2,5,8,11-tetraone (**LQ9**)*

**LQ9** was obtained following the procedure for **LQ18** in 56% yield. $[\alpha]_D^{28}$ = -16.6 (*c* 0.15, $CHCl_3$); IR (KBr) $\nu_{max}$ 3581, 3465, 1738, 1651, 1246, 1046, 739 $cm^{-1}$; $^1H$ NMR (600 MHz, $CDCl_3$)

$\delta$ 7.40−7.28 (m, 5H), 7.27−7.04 (m, 5H), 6.67 (s, 1H), 6.38−6.27 (m, 1H), 6.19 (d, *J* = 7.8 Hz, 1H), 6.14 (d, *J* = 10.8 Hz, 1H), 5.94 (s, 1H), 5.86 (dd, *J* = 15.0, 5.4 Hz, 1H), 4.72−4.63 (m, 1H), 4.54 (d, *J* = 8.4 Hz, 1H), 4.47 (d, *J* = 11.4 Hz, 1H), 3.72−3.66 (m, 1H), 3.20 (s, 3H), 3.12 (s, 3H), 3.05 (d, *J* = 6.6 Hz, 1H), 2.96 (dd, *J* = 13.8, 7.8 Hz, 1H), 2.85 (dd, *J* = 13.8, 6.6 Hz, 1H), 2.75−2.66 (m, 1H), 2.17−2.01 (m, 3H), 1.74 (s, 3H), 1.65−1.59 (m, 1H), 1.52 (s, 3H), 1.38−1.28 (m, 2H), 1.08 (s, 3H), 1.06 (d, *J* = 6.6 Hz, 3H), 1.03−0.96 (m, 1H), 0.88 (t, *J* = 7.2 Hz, 3H), 0.86−0.78 (m, 1H), 0.68 (d, *J* = 6.6 Hz, 3H); $^{13}$C NMR (150 MHz, $CDCl_3$) $\delta$ 170.8 (C=O), 170.6 (C=O) 169.6 (C=O), 169.0 (C=O), 138.2, 136.5, 135.9, 134.1, 129.1, 128.8, 128.5, 128.2, 128.0, 127.2, 126.8, 126.3, 84.2, 80.3, 72.2, 61.8, 60.7, 60.5, 58.6, 56.0, 54.4, 41.8, 39.3, 31.5, 29.9, 29.7, 26.7, 26.6, 24.4, 15.6, 15.2, 11.5, 11.3, 10.4; HRMS (ESI): calcd for $C_{42}H_{57}N_3O_8Na^+$ [M+$Na^+$] 754.4038, found 754.4068.

*(3S,6R,9S,12E,15R,16E,18E,20R,21S)-6-Benzyl-3,9-diisopropyl-15-methoxy-10,12,16,20-tetramethyl-21-phenyl-1-oxa-4,7,10-triazacyclohenicosa-12,16,18-triene-2,5,8,11-tetraone (**LQ10**)*

**LQ10** was obtained following the procedure for **LQ18** in 65% yield. $[\alpha]_D^{28}$ = -63 (*c* 0.1, $CHCl_3$); IR (KBr) $\nu_{max}$ 3679, 3309, 3022, 1742, 1686, 1216, 759 $cm^{-1}$; $^1$H NMR (600 MHz, $CDCl_3$) $\delta$ 7.40−7.11 (m, 10H), 6.93 (d, *J* = 8.4 Hz, 1H), 6.48 (d, *J* = 9.0 Hz, 1H), 6.29 (dd, *J* = 15.0, 12.0 Hz, 1H), 6.09 (s, 1H), 5.86 (d, *J* = 10.8 Hz, 1H), 5.77 (dd, *J* = 15.6, 4.8 Hz, 1H), 5.43 (t, *J* = 7.2 Hz, 1H), 4.67−4.55 (m, 2H), 4.51 (d, *J* = 11.4 Hz, 1H), 3.55 (dd, *J* = 10.8, 2.4 Hz, 1H), 3.19 (s, 3H), 3.09 (dd, *J* = 13.2, 9.6 Hz, 1H), 2.92 (dd, *J* = 13.8, 6.0 Hz, 1H), 2.68 (s, 3H), 2.64−2.52 (m, 2H), 2.42−2.35 (m, 1H), 2.35−2.27 (m, 1H), 2.25−2.15 (m, 1H), 1.82 (s, 3H), 1.75 (s, 3H), 1.03 (d, *J* = 6.6 Hz, 3H), 0.93 (d, *J* = 6.6 Hz, 3H), 0.86 (d, *J* = 6.6 Hz, 3H), 0.62 (d, *J* = 6.6 Hz, 3H), 0.45 (d, *J* = 6.6 Hz, 3H); $^{13}$C NMR (150 MHz, $CDCl_3$) $\delta$ 175.5 (C=O), 170.8 (C=O), 170.5 (C=O), 170.4 (C=O), 139.3, 136.6, 136.3, 135.1, 133.4, 129.2, 129.2, 128.7, 128.5, 128.2, 127.6, 126.8, 125.8, 125.5, 85.9, 78.0, 61.6, 56.0, 55.8, 54.6, 42.3, 36.9, 32.1, 31.8, 31.3, 24.8, 19.8, 19.0, 18.4, 16.2, 14.4, 11.1, 9.7; HRMS (ESI): calcd for $C_{41}H_{55}N_3O_6Na^+$ [M+$Na^+$] 708.3983, found 708.3993.

*(3S,6R,9S,12E,15R,16E,18E,20R,21S)-6-(3,5-Dichloro-4-hydroxybenzyl)-3,9-diisopropyl-15-methoxy-10,12,16,20-tetramethyl-21-phenyl-1-oxa-4,7,10-triazacyclohenicosa-12,16,18-triene-2,5,8,11-tetraone (**LQ11**)*

**LQ11** was obtained following the procedure for **LQ18** in 64% yield. $[\alpha]_D^{28}$ = -21 (*c* 0.1, $CHCl_3$); IR (KBr) $\nu_{max}$ 3682, 3657, 3295, 2927, 1741, 1688, 1213, 1148, 760 $cm^{-1}$; $^1$H NMR (600 MHz, $CDCl_3$) $\delta$ 7.40−7.20 (m, 5H), 7.15 (s, 1H), 6.97 (d, *J* = 8.4 Hz, 1H), 6.62 (d, *J* = 9.0 Hz, 1H), 6.30 (dd, *J* = 15.6, 10.8 Hz, 1H), 6.10 (s, 1H), 5.85 (d, *J* = 10.8 Hz, 1H), 5.77 (dd, *J* = 15.6, 5.4 Hz, 1H), 5.47−5.37 (m, 1H), 4.62 (dd, *J* = 8.4, 3.0 Hz, 1H), 4.56−4.47 (m, 2H), 3.56 (dd, *J* = 10.8, 3.0 Hz, 1H), 3.19 (s, 3H), 3.05 (dd, *J* = 13.2, 9.6 Hz, 1H), 2.77 (dd, *J* = 13.8, 5.4 Hz, 1H), 2.67 (s, 3H), 2.64−2.51 (m, 2H), 2.42−2.29 (m, 2H), 2.29−2.21 (m, 1H), 1.80 (s, 3H), 1.76 (s, 3H), 1.73−1.64 (m, 2H), 1.04 (d, *J* = 7.2 Hz, 3H), 0.97 (d, *J* = 6.6 Hz, 3H), 0.87 (d, *J* = 6.6 Hz, 3H), 0.69 (d, *J* =

6.6 Hz, 3H), 0.50 (d, *J* = 6.6 Hz, 3H); $^{13}$C NMR (150 MHz, $CDCl_3$) $\delta$ 175.7 (C=O), 171.7 (C=O), 170.7 (C=O), 169.4 (C=O), 146.7, 139.1, 136.2, 135.3, 133.3, 130.2, 129.5, 129.0, 128.7, 128.2, 127.9, 127.7, 125.9, 125.5, 120.9, 85.7, 78.1, 67.8, 61.8, 55.9, 54.3, 50.3, 42.3, 42.0, 35.4, 32.3, 31.8, 24.9, 24.7, 23.0, 21.8, 19.9, 18.5, 14.4, 11.3, 10.0; HRMS (ESI): calcd for $C_{41}H_{53}Cl_2N_3O_7Na^+$ [M+$Na^+$] 792.3153, found 792.3166.

*(1R,4S,7R,10S,13S,14R,15E,17E,19R,21S)-4-((S)-Sec-butyl)-7-(4-hydroxy-3-methoxybenzyl)-10-(2-hydroxypropan-2-yl)-19-methoxy-1,3,14,18-tetramethyl-13-phenyl-12,22-dioxa-3,6,9-triazabicyclo[19.1.0]docosa-15,17-diene-2,5,8,11-tetraone (**LQ12**)*

**LQ12** was obtained following the procedure for **LQ18** in 52% yield. $[\alpha]_D^{28}$ = -14.3 (*c* 0.1, $CHCl_3$); IR (KBr) $\nu_{max}$ 3632, 3527, 3300, 1736, 1700, 1216, 759 $cm^{-1}$; $^1$H NMR (600 MHz, $CDCl_3$) $\delta$ 7.40−7.23 (m, 5H), 6.77 (d, *J* = 7.8 Hz, 1H), 6.72 (s, 2H), 6.68 (d, *J* = 6.6 Hz, 1H), 6.64 (d, *J* = 7.8 Hz, 1H), 6.33 (dd, *J* = 13.8, 10.8 Hz, 1H), 6.19 (d, *J* = 8.4 Hz, 1H), 6.13 (d, *J* = 10.8 Hz, 1H), 5.93 (d, *J* = 3.6 Hz, 1H), 5.86 (d, *J* = 5.4 Hz, 1H), 5.84 (d, *J* = 5.4 Hz, 1H), 5.50 (s, 1H), 4.62 (q, *J* = 7.2 Hz, 1H), 4.55 (d, *J* = 8.4 Hz, 1H), 4.48 (d, *J* = 11.4 Hz, 1H), 3.84 (s, 3H), 3.69 (dd, *J* = 9.6, 3.0 Hz, 1H), 3.20 (s, 3H), 3.13 (s, 3H), 3.05 (dd, *J* = 9.0, 3.0 Hz, 1H), 2.84 (d, *J* = 7.2 Hz, 1H), 2.74−2.65 (m, 1H), 2.22−2.15 (m, 1H), 2.15−2.05 (m, 2H), 1.75 (s, 3H), 1.65−1.61 (m, 3H), 1.11 (s, 3H), 1.07 (s, 3H), 1.06 (s, 3H), 0.89 (t, *J* = 7.2 Hz, 3H), 0.74 (d, *J* = 6.0 Hz, 3H); $^{13}$C NMR (150 MHz, $CDCl_3$) $\delta$ 170.8 (C=O), 170.6 (C=O), 169.5 (C=O), 169.0 (C=O), 146.7, 144.7, 138.1, 135.9, 134.1, 128.5, 128.2, 128.2, 128.0, 126.7, 126.3, 122.0, 114.4, 111.2, 84.2, 80.3, 72.2, 61.8, 60.7, 60.5, 58.6, 56.0, 55.9, 54.7, 41.8, 39.0, 31.6, 29.9, 29.7, 26.8, 26.4, 24.4, 22.7, 15.6, 15.3, 14.1, 11.5, 11.2, 10.5; HRMS (ESI): calcd for $C_{43}H_{59}N_3O_{10}Na^+$ [M+$Na^+$] 800.4093, found 800.4107.

*(3S,6R,9S,12E,15R,16E,18E,20R,21S)-6-(3,5-Dichloro-4-hydroxybenzyl)-3-isobutyl-9-isopropyl-15-methoxy-10,12,16,20-tetramethyl-21-phenyl-1-oxa-4,7,10-triazacyclohenicosa-12,16,18-triene-2,5,8,11-tetraone (**LQ13**)*

**LQ13** was obtained following the procedure for **LQ18** in 62% yield. $[\alpha]_D^{28}$ = -22.7 (*c* 0.1, $CHCl_3$); IR (KBr) $\nu_{max}$ 3757, 3694, 3043, 1777, 1742, 1217, 761 $cm^{-1}$; $^1$H NMR (600 MHz, $CDCl_3$) $\delta$ 7.33 (t, *J* = 7.2 Hz, 2H), 7.28 (d, *J* = 7.2 Hz, 1H), 7.22 (d, *J* = 7.2 Hz, 2H), 7.13 (s, 2H), 6.93 (d, *J* = 8.4 Hz, 1H), 6.66 (d, *J* = 8.4 Hz, 1H), 6.30 (dd, *J* = 14.4, 10.8 Hz, 1H), 6.06 (s, 1H), 5.86 (d, *J* = 10.2 Hz, 1H)., 5.84−5.80 (m, 1H), 5.77 (dd, *J* = 15.0, 4.8 Hz, 1H), 5.46 (t, *J* = 7.2 Hz, 1H), 4.64−4.54 (m, 1H), 4.54−4.43 (m, 2H), 3.57 (dd, *J* = 10.8, 2.4 Hz, 1H), 3.20 (s, 3H), 3.03 (dd, *J* = 13.8, 9.6 Hz, 1H), 2.77 (dd, *J* = 13.8, 5.4 Hz, 1H), 2.70 (s, 3H). 2.65−2.51 (m, 2H), 2.44−2.26 (m, 2H), 1.81 (s, 3H), 1.76 (s, 3H), 1.58−1.52 (m, 1H), 1.41−1.33 (m, 2H), 1.02 (d, *J* = 6.6 Hz, 3H), 0.96 (d, *J* = 6.6 Hz, 3H), 0.87 (d, *J* = 6.6 Hz, 3H), 0.85 (d, *J* = 6.6 Hz, 3H), 0.76 (d, *J* = 6.6 Hz, 3H); $^{13}$C NMR (150 MHz, $CDCl_3$) $\delta$ 175.7 (C=O), 171.7 (C=O), 170.7 (C=O), 169.4 (C=O), 146.7,

139.1, 136.2, 135.1, 133.3, 130.2, 129.5, 129.0, 128.5, 128.2, 128.0, 127.7, 125.9, 125.6, 120.9, 85.7, 78.1, 67.8, 61.8, 55.9, 54.3, 50.3, 42.3, 42.0, 35.4, 32.3, 31.8, 24.9, 24.7, 23.0, 21.8, 19.9, 18.5, 14.4, 11.3, 10.0; HRMS (ESI): calcd for $C_{42}H_{55}Cl_2N_3O_7Na^+$ [M+$Na^+$] 806.3309, found 806.3332.

*(3S,6R,9S,12E,15R,16E,18E,20R,21S)-6-(4-Hydroxybenzyl)-3,9-diisopropyl-15-methoxy-10,12,16, 20-tetramethyl-21-phenyl-1-oxa-4,7,10-triazacyclohenicosa-12,16,18-triene-2,5,8,11-tetraone* ***(LQ14)***

**LQ14** was obtained following the procedure for **LQ18** in 64% yield. $[\alpha]_D^{28}$ = -21.5 (*c* 0.19, $CHCl_3$); IR (KBr) $\nu_{max}$ 3461, 3391, 1639, 1092, 738, 703 $cm^{-1}$; $^1$H NMR (600 MHz, $CDCl_3$) $\delta$ 7.37−7.18 (m, 5H), 7.06 (dd, *J* = 8.4, 2.4 Hz, 2H), 6.93 (dd, *J* = 8.4, 3.6 Hz, 1H), 6.71 (d, *J* = 8.4 Hz, 2H), 6.59 (dd, *J* = 9.0, 4.8 Hz, 1H), 6.30 (dd, *J* = 15.0, 10.8 Hz, 1H), 6.09 (s, 1H), 5.86 (d, *J* = 10.8 Hz, 1H), 5.78 (dd, *J* = 15.6, 4.8 Hz, 1H), 5.43 (t, *J* = 7.2 Hz, 1H), 4.62 (dd, *J* = 8.4, 3.0 Hz, 1H), 4.56 (q, *J* = 8.4, 1H), 4.51 (d, *J* = 11.4 Hz, 1H), 3.56 (dd, *J* = 10.2, 3.0 Hz, 1H), 3.20 (s, 3H), 3.01 (dd, *J* = 13.8, 9.0 Hz, 1H), 2.85 (dd, *J* = 13.8, 6.4 Hz, 1H), 2.69 (s, 3H). 2.64−2.52 (m, 2H), 2.43−2.35 (m, 1H), 2.35−2.27 (m, 1H), 2.27−2.18 (m, 1H), 1.81 (s, 3H), 1.75 (s, 3H), 1.03 (d, *J* = 6.8 Hz, 3H), 0.92 (d, *J* = 6.4 Hz, 3H), 0.85 (d, *J* = 6.6 Hz, 3H), 0.69 (d, *J* = 6.9 Hz, 3H), 0.51 (d, *J* = 6.9 Hz, 3H); $^{13}$C NMR (150 MHz, $CDCl_3$) $\delta$ 175.5 (C=O), 170.9 (C=O), 170.6 (C=O), 170.6 (C=O), 139.3, 136.3, 135.1, 133.3, 130.4, 130.4, 128.6, 128.2, 127.8, 127.8, 127.6, 125.8, 125.5, 115.4, 85.9, 78.0, 61.7, 56.1, 55.8, 54.7, 42.4, 36.0, 32.2, 31.8, 31.4, 24.9, 19.9, 19.1, 18.4, 16.3, 14.4, 11.2, 9.8; HRMS (ESI): calcd for $C_{41}H_{55}N_3O_7Na^+$ [M+$Na^+$] 724.3932, found 724.3925.

*(3S,6R,9S,12E,15R,16E,18E,20R,21S)-6-(3,5-Dichloro-4-hydroxybenzyl)-16-ethyl-3,9-diisopropyl -15-methoxy-10,12,20-trimethyl-21-phenyl-1-oxa-4,7,10-triazacyclohenicosa-12,16,18-triene-2,5, 8,11-tetraone (****LQ15****)*

**LQ15** was obtained following the procedure for **LQ18** in 60% yield. $[\alpha]_D^{28}$ = -90 (*c* 0.3, $CHCl_3$); IR (KBr) $\nu_{max}$ 3680, 3078, 2903, 1750, 1708, 1384, 1242, 916 $cm^{-1}$; $^1$H NMR (600 MHz, $CDCl_3$) $\delta$ 7.40−7.19 (m, 5H), 7.12 (s, 2H), 6.90 (d, *J* = 8.4 Hz, 1H), 6.68 (d, *J* = 9.0 Hz, 1H), 6.33 (dd, *J* = 14.4, 10.8 Hz, 1H), 6.01 (s, 1H), 5.82 (d, *J* = 10.8 Hz, 1H), 5.84−5.75 (m, 1H), 5.70 (dd, *J* = 15.0, 6.0 Hz, 1H), 5.43 (t, *J* = 7.8 Hz, 1H), 4.60 (dd, *J* = 9.0, 3.6 Hz, 1H), 4.57−4.51 (m, 1H), 4.49 (d, *J* = 11.4 Hz, 1H), 3.65 (dd, *J* = 9.6, 2.4 Hz, 1H), 3.26 (s, 1H), 3.05 (dd, *J* = 13.8, 9.6 Hz, 1H), 2.77 (dd, *J* = 13.2, 5.4 Hz, 1H), 2.67 (s, 3H), 2.64−2.56 (m, 2H), 2.48−2.38 (m, 1H), 2.36−2.28 (m, 1H), 2.28−2.20 (m, 1H), 2.21 (q, *J* = 7.8 Hz, 2H), 1.82 (s, 3H), 1.09 (t, *J* = 7.5 Hz, 3H), 1.00 (d, *J* = 6.8 Hz, 3H), 0.95 (d, *J* = 6.3 Hz, 3H), 0.86 (d, *J* = 6.5 Hz, 3H), 0.72 (d, *J* = 6.8 Hz, 3H), 0.56 (d, *J* = 6.8 Hz, 3H).; $^{13}$C NMR (150 MHz, $CDCl_3$) $\delta$ 175.6 (C=O), 170.7 (C=O), 170.7 (C=O) , 170.1 (C=O), 146.6, 140.8, 138.8, 136.4, 132.9, 130.1, 129.0, 128.2, 128.1, 127.7, 127.6, 126.0, 125.7, 120.9, 84.4, 78.6, 61.9, 56.3, 56.2, 54.3, 42.5, 35.4, 32.2, 31.5, 31.2, 29.7, 24.9, 20.7, 19.9, 19.0,

18.5, 16.5, 14.5, 14.4, 11.1; HRMS (ESI): calcd for $C_{42}H_{55}Cl_2N_3O_7Na^+$ [M+$Na^+$] 806.3309, found 806.3336.

*(3S,6R,9S,12E,15R,16E,18E,21S)-6-Benzyl-3,9-diisopropyl-15-methoxy-10,12,16-trimethyl-21-phenyl-1-oxa-4,7,10-triazacyclohenicosa-12,16,18-triene-2,5,8,11-tetraone (**LQ17**)*

**LQ17** was obtained following the procedure for **LQ18** in 70% yield. $[\alpha]_D^{28}$ = -52 (*c* 0.3, $CHCl_3$); IR (KBr) $\nu_{max}$ 3564, 3520, 3482, 1644, 700, 665, 607 $cm^{-1}$; $^1H$ NMR (600 MHz, $CDCl_3$) $\delta$ 7.34−7.19 (m, 9H), 7.18−7.13 (m, 1H), 6.95 (t, *J* = 9.0 Hz, 1H), 6.48 (t, *J* = 7.8 Hz, 1H), 6.37 (dd, *J* = 14.4, 11.4 Hz, 1H), 5.89 (d, *J* = 11.4 Hz, 1H), 5.82 (d, *J* = 10.8 Hz, 1H), 5.59-5.49 (m, 1H), 5.40 (t, *J* = 7.2 Hz, 1H), 4.62−4.55 (m, 1H), 4.53 (d, *J* = 11.4 Hz, 1H), 4.43 (dd, *J* = 8.4, 3.6 Hz, 1H), 3.54 (dd, *J* = 10.8, 2.4 Hz, 1H), 3.18 (s, 3H), 3.07 (dd, *J* = 13.2, 9.6 Hz, 1H), 2.91 (dd, *J* = 13.8, 6.0 Hz, 1H), 2.76−2.67 (m, 1H), 2.64 (s, 3H), 2.61−2.53 (m, 1H), 2.53−2.46 (m, 1H), 2.40−2.28 (m, 2H), 1.95−1.84 (m, 2H), 1.82 (s, 3H), 1.75 (s, 3H), 0.95 (d, *J* = 6.6 Hz, 1H), 0.86 (d, *J* = 6.6 Hz, 1H), 0.45 (d, *J* = 6.6 Hz, 1H), 0.30 (d, *J* = 7.2 Hz, 1H).; $^{13}C$ NMR (150 MHz, $CDCl_3$) $\delta$ 175.5 (C=O), 171.1 (C=O), 170.5 (C=O), 170.2 (C=O), 139.9, 136.6, 135.7, 133.6, 129.5, 129.2, 129.0, 128.6, 128.5, 128.5, 128.4, 127.1, 126.7, 126.5, 86.1, 75.8, 61.5, 55.9, 55.8, 54.8, 40.3, 36.8, 32.1, 31.9, 31.3, 24.7, 19.8, 18.5, 18.3, 16.3, 14.3, 10.5.; HRMS (ESI): calcd for $C_{40}H_{53}N_3O_6Na^+$ [M+$Na^+$] 694.3827, found 694.3812.

4.4 Cell viability

Cancer cell viability after the treatment of **LQ2-18** and nannocystin A was assessed by MTT assay following manufacturer's suggestion. **LQ2-18** and nannocystin A were dissolved in pure DMSO to prepare 10 mM stocking solution and diluted with culture medium. Cells (A549, HCT-116, MCF-7, A375, SH-SY-5Y, and MDA-MB-231) at a density of $5 \times 10^3$ per well were seeded in 96-well plates and cultured overnight, which were then treated with either vehicle (1% DMSO PBS buffer) or desired concentrations of **LQ2-18** and nannocystin A (10, 1, 0.1, 0.01, 0.001, and 0.0001 μM) for 72 h at 37 °C. Then, culturing medium was discarded and 100 μL fresh media containing 0.5 mg/mL MTT was added. After 4 h of incubation at 37 °C, the supernatant was removed and 100 μL DMSO was added to each well with the aid of gentle shaking. The absorbance of the each well was measured at 570 nm in a microplate reader (Bio-Rad Laboratories). At last, the resultant $OD_{570}$ nm values were expressed as $IC_{50}$ values, which were the mean values derived from three independent experiments.

4.5 Colony formation assay

A549 cells were seeded in 6-well plates, each well contained 2 mL medium with 500 A549 cells and incubated for 24 h. Then **LQ18** (5, 10 and 20 nM) and nannocystin A (10 nM) in fresh medium were added into the corresponding well to treat cells for a continuous 3 days, then replaced by 2 mL of drug-free medium for every 3 days. 15 days after the cell plating, cell

colonies were fixed in 95% ethanol for 15 min and stained by 0.1% crystal violet (Sigma), and dried for colonies counting.

4.6 Cell cycle

A549 cells at the density of $1 \times 10^5$ cells/well were seeded in 6-well plates and treated with **LQ18** (30, 60 and 90 nM) and nannocystin A (30 nM) for 24 h at 37 °C. Then, the cells were harvested and fixed with 70% precooled ethanol. Cells were then treated with RNase A, and stained by PI (Product #: C1052, Beyotime, Jiangsu, China). Finally, the suspended cell was analyzed with a flow cytometer (Accuri C6, BD Biosciences), a minimum total of 10,000 events were recorded.

4.7 Cell apoptosis

A549 cells at a density of $2 \times 10^5$ cells/well were seeded on each well of 6-well plates and allowed to grow overnight. Then the cells were treated with **LQ18** (30, 60 and 90 nM) and nannocystin A (30 nM) for 12 h (dose-dependent experiment), or cells were treated with **LQ18** (60 nM) for 6, 12, and 24 h (time-dependent experiment), while cells without treatment were used as control group. The treated cells were trypsinized and washed with cold PBS for three times, then centrifuged at 1200 rpm for 5 min. The supernatants were discarded, and the cells were stained by an Annexin-V-fluorescein isothiocyanate (FITC) kit with the binding buffer for 15 min. Subsequently, the cells were then labeled by PI and the apoptotic cells were measured by a flow cytometer (Accuri C6), data were analyzed with BD Accuri C6 Plus.

4.8 Western blotting

After the treatment of A549 cells with **LQ18** (30, 60 and 90 nM) and nannocystin A (30 nM) for 24 h, the total proteins from A549 cells were extracted and their concentrations were balanced to the same level by using BCA protein assay reagent (Beyotime, Jiangsu, China), followed by 8 min of protein denaturation with SDS loading buffer at 100 °C. Proteins (30 μg) were separated by sodium dodecyl sulfate-polyacrylamide electrophoresis (SDS-PAGE) and transferred onto polyvinylidene fluoride (PVDF) membranes, which were blocked with 5 mL of 5% fat-free dry milk in 1 × Tris-buffered saline (TBS) containing 0.05% Tween 20 for 2 h. Then the membranes were incubated with caspase-3 (Beyotime, no: AC030), caspase-9 (Beyotime, no: AC062), Bcl-2 (Beyotime, no: AB112), Bad (Beyotime, no: AB008) and β-actin (Beyotime, no: AF0003), and eEF1A1 (proteintech) antibodies at 4 °C for overnight, followed by treatment of secondary horseradish-peroxidase-conjugated anti-rabbitIgG (Beyotime, no: A0208) for 2 h. Membranes were finally scanned in a ChemiDoc MP Imaging System (Bio-Rad) after 2 min incubation in Clarity Western ECL Substrate (Bio-Rad).

4.9 Statistical analysis

Data were reported as means ± SD. Statistical analysis was performed using GraphPad Prism

version. *$p < 0.05$ was considered as statistically significant.

**Acknowledgments**

We thank the financial support from National Natural Science Foundation of China (No. 21807008, 21572027).

**References**

1. A.L. Harvey, R.E. Ebel, R.J. Quinn, The re-emergence of natural products for drug discovery in the genomics era, Nat. Rev. Drug Discov. 14 (2015) 111–129.
2. D.A. Dias, S. Urban, U. Roessner, A historical overview of natural products in drug discovery, Metabolites 2 (2012) 303–333.
3. A.L. Harvey, Natural products in drug discovery, Drug Discov. Today 13 (2008) 894–901.
4. D.J. Newman, G.M. Cragg, Natural products as sources of new drugs over the 30 years from 1981 to 2010, J. Nat. Prod. 75 (2012) 311–335.
5. H. Hoffmann, H. Kogler, W. Heyse, H. Matter, M. Caspers, D. Schummer, C. Klemke-Jahn, A. Bauer, G. Penarier, L. Debussche, M. Brönstrup, Discovery, structure elucidation, and biological characterization of nannocystin A, a macrocyclic myxobacterial metabolite with potent antiproliferative properties, Angew. Chem. Int. Ed. 54 (2015) 10145–10148.
6. P. Krastel, S. Roggo, M. Schirle, N.T. Ross, F. Perruccio, P. Aspesi, J.T. Aust, K. Buntin, D. Estoppey, B. Liechty, F. Mapa, K. Memmert, H. Miller, X. W. Pan, R. Riedl, C. Thibaut, J. Thomas, T. Wagner, E. Weber, X. B. Xie, E.K. Schmitt, D. Hoepfner, Nannocystin A: an elongation factor 1 inhibitor from Myxobacteria with differential anti-cancer properties, Angew. Chem. Int. Ed. 54 (2015) 10149–10154.
7. J. Condeelis, Elongation factor 1 alpha, translation and the cytoskeleton, Trends Biochem. Sci. 20 (1995) 169−170.
8. M.K. Mateyak, T.G. Kinzy, EEF1A: thinking Outside the Ribosome, J. Bio. Chem. 285 (2010) 21209–21213.
9. A. Lamberti, M. Caraglia, O. Longo, M. Marra, A. Abbruzzese, P. Arcari, The translation elongation factor 1A in tumorigenesis, signal transduction and apoptosis, Amino Acids 26 (2004) 443−448.
10. A. Duttaroy, D. Bourbeau, X.L. Wang, E. Wang, Apoptosis rate can be accelerated or decelerated by overexpression or reduction of the level of elongation factor-1a, Exp. Cell Res. 238 (1998) 168−176.
11. G. Van Goietsenoven, J. Hutton, J.P. Becker, B. Lallemand, F. Robert, F. Lefranc, C. Pirker, G. Vandenbussche, P. Van Antwerpen, A. Evidente, W. Berger, M. Prevost, J. Pelletier, R. Kiss, T. Goss Kinzy, A. Kornienko, V. Mathieu, Targeting of eEF1A with amaryllidaceae isocarbostyrils as a strategy to combat melanomas, FASEB J. 24 (2010) 4575−4584.

12. Q. Liu, P. Hu, Y. He, Asymmetric total synthesis of nannocystin A, J. Org. Chem. 82 (2017) 9217−9222.
13. L. Liao, J. Zhou, Z. Xu, T. Ye, Concise total synthesis of nannocystin A, Angew. Chem. Int. Ed. 55 (2016) 13263−13266.
14. J. Huang, Z. Wang, Total syntheses of nannocystins A and A0, two elongation factor 1 inhibitors, Org. Lett. 18 (2016) 4702−4705.
15. Z. Yang, X. Xu, C.-H. Yang, Y. Tian, X. Chen, L. Lian, W. Pan, X. Su, W. Zhang, Y. Chen, Total synthesis of nannocystin A, Org. Lett. 18 (2016) 5768−5770.
16. Y.F. Tian, X.L. Xu, Y.H. Ding, X. Hao, Y.J. Bai, Y. Tang, X.M. Zhang, Q.Y. Li, Z.T. Yang, W.C. Zhang, Y. Chen, Synthesis and biological evaluation of nannocystin analogues toward understanding the binding role of the (2R,3S)-Epoxide in nannocystin A, Eur. J. Med. Chem. 150 (2018) 626−632.
17. Y.F. Tian, Y.H. Ding, X.L. Xu, Y.J. Bai, Y. Tang, X. Hao, W.C. Zhang, Y. Chen, Total synthesis and biological evaluation of nannocystin analogues modified at the polyketide phenyl moiety, Tetrahedron Lett. 59 (2018) 3206–3209.
18. N. Zhang, Z.M. Yu, X.H. Yang, Y. Zhou，J. Wang, S.L. Zhang, M.W. Wang, Y. He, Synthesis, biological evaluation and structure-activity relationship of a novel class of PI3Kα H1047R mutant inhibitors, Eur. J. Med. Chem. 158 (2018) 707−719.
19. N. Zhang, Z.M. Yu, X.H. Yang, Y. Zhou, Q. Tang, P. Hu, J. Wang, S.L. Zhang, M.W. Wang, Y. He, Difuran-substituted quinoxalines as a novel class of PI3Kα H1047R mutant inhibitors: synthesis, biological evaluation and structure-activity relationship, Eur. J. Med. Chem. 157 (2018) 37−49.
20. B. Xu, Z.M. Yu, S.C. Xiang, Y.S. Li, S.L. Zhang, Y. He, Rational design of mitochondria-targeted pyruvate dehydrogenase kinase 1 inhibitors with improved selectivity and antiproliferative activity, Eur. J. Med. Chem. 155 (2018) 275−284.
21. N. Zhang, Z.M. Yu, X.H. Yang, P. Hu, Y. He, Synthesis of novel ring-contracted artemisinin dimers with potent anticancer activities, Eur. J. Med. Chem. 150 (2018) 829–840.
22. X.H. Yang, J.S. Gao, J. Guo, Z.M. Zhao, S.L. Zhang, Y. He, Anti-lung cancer activity and inhibitory mechanisms of a novel Calothrixin A derivative, Life Sciences 219 (2019) 20–30.
23. Z.H. Lin, X.B. Xu, S. Zhao, X.H. Yang, J. Guo, Q. Zhang, C.M. Jing, S. Chen, Y. He, Total synthesis and antimicrobial evaluation of natural albomycins against clinical pathogens, Nat. Commun. 9 (2018) 3445.
24. N. Schläger, A. Kirschning, Substrate-controlled stereoselectivity in the Yamamoto aldol reaction, Org. Biomol. Chem. 10 (2012) 7721−7729.
25. V.P. Kumar, S. Chandrasekhar, Enantioselective synthesis of pladienolide B and truncated analogues as new anticancer agents, Org. Lett. 15 (2013) 3610−3613.

26. F.-X. Felpin, J. Lebreton, A highly stereoselective asymmetric synthesis of (−)-Lobeline and (−)-Sedamine, J. Org. Chem. 67 (2002) 9192−9199.
27. M.T. Gieseler, M. Kalesse, Asymmetric vinylogous mukaiyama aldol reaction of aldehyde-derived dienolates, Org. Lett. 13 (2011) 2430−2432.
28. N. Qi, S.R. Allu, Z.L. Wang, Q. Liu, J. Guo, Y. He, Asymmetric total syntheses of aetheramides and their stereoisomers: stereochemical assignment of Aetheramides, Org. Lett. 18 (2016) 4718−4721.
29. S. Shirokawa, M. Kamiyama, T. Nakamura, M. Okada, A. Nakazaki, S. Hosokawa, S. Kobayashi, Remote asymmetric induction with vinylketene silyl N,O-acetal, J. Am. Chem. Soc. 126 (2004) 13604−13605.
30. M. Harada, K.N. Asaba, M. Iwai, N. Kogure, M. Kitajima, H. Takayama, Asymmetric total synthesis of an iboga-type indole alkaloid, Voacangalactone, newly isolated from *Voacanga africana*, Org. Lett. 14 (2012) 5800−5803.

## Highlights

► The SAR of nannocystin A analogues was established based on the MTT assay and Western blotting analysis

► **LQ18** exhibited potent antiproliferative activities with $IC_{50}$ values ranging from 4.3 to 48 nM against tested cancer cell lines

► **LQ18** inhibited eEF1A expression in A549 cell line